

B_c Exclusive Decays to Charmonia and Light Mesons in QCD Factorization at Next-to-Leading Order Accuracy

Cong-Feng Qiao^{a1}, Peng Sun^{b,c2}, Deshan Yang^{a3} and Rui-Lin Zhu^{a4}

^a *Department of Physics, University of Chinese Academy of Sciences
YuQuan Road 19A, Beijing 100049, China*

^b *Center for High-Energy Physics, Peking University, Beijing 100871, China*

^c *Nuclear Science Division, LBNL, Berkeley, CA 94720, USA*

Abstract

In this paper, the branching ratios of B_c decays to S-wave charmonia along with light mesons including π , ρ , k and k^* up to twist-3 light-cone distribution amplitudes at next-to-leading order (NLO) are performed both in non-relativistic QCD and in light-cone QCD framework. Renormalization scale dependence for the decay widths is obviously depressed at NLO correction, hence the theoretic uncertainty is correspondingly reduced. Numerical results show that NLO QCD corrections markedly enhanced the branching ratios with a K factor of 1.75 for $B_c^\pm \rightarrow \eta_c \pi^\pm$ and 1.31 for $B_c^\pm \rightarrow J/\Psi \pi^\pm$, which can now be checked in the LHCb experiment. Besides, in the heavy quark limit $m_b \rightarrow \infty$, the factorization is shown to hold at two scenarios: non-relativistic (NR) factorization scheme and light-cone (LC) factorization scheme. We note that the annihilation diagrams contribute trivially in this limit, and the leading order contribution in $z = m_c/m_b$ expansion comes from form factors and hard spectator interactions. Analytic investigations ensure that the comparison for the processes within between NRQCD \otimes NRQCD \otimes SCET and SCET \otimes SCET \otimes SCET is more clear. At last, some related phenomenologies are also discussed.

¹E-mail:qiaocf@gucas.ac.cn

²E-mail:sunp@pku.edu.cn

³E-mail:yangds@gucas.ac.cn

⁴E-mail:zhuruilin09@mails.gucas.ac.cn

Contents

1	Introduction	1
2	The theoretical frame	2
3	The non-relativistic factorization scheme	3
3.1	Tree-level results	3
3.2	One-loop results	5
3.2.1	$T_0^{(1)}$	5
3.2.2	$T_8^{(1)}$	9
4	The light-cone factorization scheme	10
4.1	Definition and matching	10
4.2	The LC's results	13
4.3	Comparison with NR scheme	14
5	The phenomenological studies	15
6	Conclusions	18
A	Twist-2 and -3 LCDA for light pseudoscalar and vector mesons and non-relativistic projection operators for heavy quarkonia	19
B	Renormalization and infre-red subtractions	20
C	Master integrals	21
D	Formulas for contributions of non-factorizable diagrams	23
E	The NLO B_c to charmonia transition form factors	26

1 Introduction

B_c with its excited states is the unique meson containing two different kinds of heavy flavor. The studies on the production and decay of B_c can shed light on the understanding of the strong interaction in such a unique system. In contrast to other B mesons just with one heavy flavor which can be produced massively through the e^+e^- and ep collisions, the cross section for B_c^- production is suppressed owing to the associated production of two additional heavy quarks c and \bar{b} [1].

However, B_c can be produced remarkably at the hadron colliders. Since the first discovery of B_c was reported in 1998 by the CDF collaboration at the Tevatron [2], there are continuous measurements of its mass in different detectors via two different channels: $B_c^\pm \rightarrow J/\Psi \ell^\pm \nu_\ell$ and $B_c^\pm \rightarrow J/\Psi \pi^\pm$ [3–7]. Therein, using 1.3 fb^{-1} of integrated luminosity, the D0 collaboration measured the B_c mass with $6300 \pm 14(\text{stat}) \pm 5(\text{sys}) \text{ MeV}/c^2$ [3]. In the same year, using the data corresponding to an integrated luminosity of 2.4 fb^{-1} , with a significance that exceeds 8σ , the CDF collaboration updated the B_c mass measurement to $6275.6 \pm 2.9(\text{stat}) \pm 2.5(\text{sys}) \text{ MeV}/c^2$ [4]. Nevertheless, the intrinsic quantum numbers, angular momentum and parity of B_c has not been confirmed by experiment up to now, and the exact branching ratio for any mode of B_c decays has not been performed too. And the authors in Ref. [7] analyzed the prospects of the B_c studies of the LHCb experiment and concluded that LHC will provide a wider platform to study the intrinsic properties of B_c meson systematically. Furthermore, the ratio of branching fractions $Br(B_c^+ \rightarrow J/\Psi \pi^+ \pi^- \pi^+)/Br(B_c^+ \rightarrow J/\Psi \pi^+)$ is measured to be $2.41 \pm 0.30 \pm 0.33$ by the LHCb experiment recently [8].

We calculated the NLO QCD corrections to $B_c^\pm \rightarrow J/\Psi \pi^\pm$ for three reasons. one of them is that the cross section for B_c production at the LHC is larger than at the Tevatron by a factor of about 16 [1, 9, 10], which reaches 49.8 nb at the center-of-mass energy $\sqrt{s} = 14 \text{ TeV}$. That means around 10^{10} B_c meson per year can be anticipated at LHC. Another reason is that the hadronic mode $B_c^\pm \rightarrow J/\Psi \pi^\pm$ is one of the golden modes for the precise measurement of the intrinsic properties such as the mass, the quantum numbers and the CP violation of B_c meson, due to its clear experimental signal. And the last reason comes from the reduction of theoretic uncertainty.

Theoretically, this decay was studied within the frame of the naive factorization, potential model, pQCD method and QCD factorization in the heavy quark limit. Along the technique for the QCD factorization for the exclusive hard processes, such as π electromagnetic form-factors at the large momentum transfer and B meson decays to two light mesons, many theorists believe that the QCD factorization for $B_c^- \rightarrow J/\Psi \pi^-$ holds in the heavy quark limit generally. However, there is no complete or consistent predictions based at the next-to-leading order (NLO) in α_s so far.

Since B_c^- contains two kinds of heavy quark, namely b and c quarks, the heavy quark limit may be realized in two different scenarios. The first one is to let $m_b, m_c \rightarrow \infty$ and keep the ratio $z = m_c/m_b$ fixed; the second one is to let $m_b, m_c \rightarrow \infty$ and meanwhile $z \rightarrow 0$. Under these two different scenarios, the decay amplitude of $B_c^- \rightarrow J/\Psi(\eta_c)\pi^-$ is factorized in different ways. For the first scenario of the heavy quark limit, the factorization formula is

$$\mathcal{A}(B_c^- \rightarrow J/\Psi(\eta_c)\pi^-) \sim \Psi_{c\bar{c}}(0)\Psi_{b\bar{c}}(0) \int_0^1 dx T_H(x, \mu) \phi_\pi(x, \mu) + \mathcal{O}(1/m_b) + \mathcal{O}(v). \quad (1)$$

Here $\Psi_{c\bar{c}}(0)$ and $\Psi_{b\bar{c}}(0)$ denote the Schrödinger wave functions at origin of $J/\Psi(\eta_c)$ and B_c^- , respectively; $T_H(x, \mu)$ is the perturbatively calculable hard kernel, and $\phi_\pi(x, \mu)$ the pion's light-cone distribution amplitude (LCDA). For the second scenario, the factorization of $B_c^- \rightarrow J/\Psi(\eta_c)\pi^-$ is similar to the case of the QCD factorization for B decays to two light mesons. At the leading order of $1/m_b$, the factorization formula is

$$\begin{aligned} \mathcal{A}(B_c^- \rightarrow J/\Psi(\eta_c)\pi^-) &\rightarrow F^{B \rightarrow J/\Psi(\eta_c)}(0) \int_0^1 dx T_I(x, \mu) \phi_\pi(x, \mu) \\ &+ \int d\omega dx dy T_{II}(\omega, x, y) \phi_B(\omega) \phi_\pi(x) \phi_{J/\Psi(\eta_c)}(y) + \mathcal{O}(1/m_b) + \mathcal{O}(v). \end{aligned} \quad (2)$$

Here $F^{B \rightarrow J/\Psi(\eta_c)}(0)$ is the $B_c \rightarrow J/\Psi(\eta_c)$ transition form-factor at the large recoil; $\phi_B(\omega)$ and $\phi_{J/\Psi(\eta_c)}(y)$ are the LCDAs for B_c^- and $J/\Psi(\eta_c)$, respectively; $T_{I,II}$ are the perturbatively calculable hard kernels. In the following, we denote the factorization formula in (1) as non-relativistic (NR) factorization scheme, and the factorization formula in (2) as light-cone (LC) factorization scheme.

The following sections are organized as follows: in Sect. 2 we present a brief overview of the effective weak Hamiltonian; and in Sect. 3 and 4 we present the detailed computation in the NR and LC factorization schemes, respectively; in Sect. 5 some phenomenological predictions and discussions based our calculation are given; at last we conclude in Sect. 6.

2 The theoretical frame

In the Standard Model (SM), $B_c^- \rightarrow J/\Psi \pi^-$ occurs through W -mediated charge current process. However, since $m_W \gg m_{b,c}$, Λ_{QCD} , the large logarithm arise in the higher order strong interaction corrections. Thus, the RG-improved perturbation theory must be resorted. In the community of B physics, this turns to be the effective weak Hamiltonian method. The effective weak Hamiltonian governing $B_c^- \rightarrow J/\Psi \pi^-$ is

$$\mathcal{H}_{\text{eff}} = \frac{G_F}{\sqrt{2}} V_{ud}^* V_{cb} (C_1(\mu) Q_1(\mu) + C_2(\mu) Q_2(\mu)) , \quad (3)$$

with G_F being the Fermi constants, V_{ud} and V_{cb} the Cabibbo-Kobayashi-Maskawa (CKM) matrix-elements, $C_{1,2}(\mu)$ are perturbatively calculable Wilson coefficients, and $Q_{1,2}(\mu)$ the effective four-quark operators

$$Q_1 = \bar{d}_\alpha \gamma^\mu (1 - \gamma_5) u_\alpha \bar{c}_\beta \gamma_\mu (1 - \gamma_5) b_\beta , \quad (4a)$$

$$Q_2 = \bar{d}_\alpha \gamma^\mu (1 - \gamma_5) u_\beta \bar{c}_\beta \gamma_\mu (1 - \gamma_5) b_\alpha , \quad (4b)$$

where α, β are color indices and the summation convention over repeated indices are understood. For the conveniences of our later calculations, we will adopt another operator basis, such that

$$\mathcal{H}_{\text{eff}} = \frac{G_F}{\sqrt{2}} V_{ud}^* V_{cb} (C_0(\mu) Q_0(\mu) + C_8(\mu) Q_8(\mu)) , \quad (5)$$

with

$$Q_0 = \bar{d}_\alpha \gamma^\mu (1 - \gamma_5) u_\alpha \bar{c}_\beta \gamma_\mu (1 - \gamma_5) b_\beta , \quad (6a)$$

$$Q_8 = \bar{d}_\alpha T_{\alpha\beta}^A \gamma^\mu (1 - \gamma_5) u_\beta \bar{c}_\rho T_{\rho\lambda}^A \gamma_\mu (1 - \gamma_5) b_\lambda , \quad (6b)$$

where T^A s are the generators of the fundamental representation for $\text{SU}_C(3)$. Applying the Fierz rearrangement relation

$$T_{\alpha\beta}^A T_{\rho\lambda}^A = -\frac{1}{6} \delta_{\alpha\beta} \delta_{\rho\lambda} + \frac{1}{2} \delta_{\alpha\lambda} \delta_{\rho\beta} , \quad (7)$$

we have immediately

$$Q_0 = Q_1 , \quad Q_8 = -\frac{1}{6} Q_1 + \frac{1}{2} Q_2 . \quad (8)$$

Consequently, for the Wilson coefficients, we have

$$C_0 = C_1 + C_2/3 , \quad C_8 = 2C_2 . \quad (9)$$

Then, the decay amplitude of $B_c^- \rightarrow J/\Psi(\eta_c) \pi^-$ can be written as

$$\begin{aligned} \mathcal{A}(B_c^- \rightarrow J/\Psi(\eta_c) \pi^-) &= \langle J/\Psi(\eta_c) \pi^- | \mathcal{H}_{\text{eff}} | B_c^- \rangle \\ &= \frac{G_F}{\sqrt{2}} V_{ud}^* V_{cb} (C_0(\mu) \langle Q_0(\mu) \rangle + C_8(\mu) \langle Q_8(\mu) \rangle) . \end{aligned} \quad (10)$$

3 The non-relativistic factorization scheme

Systematically, non-relativistic QCD theory provides an rigorous factorization formalism for the annihilation and production of heavy quarkonium [11]. In this framework, it is assumed that the heavy quarkonium's production comes from two steps: a Fock state such as $|q\bar{q}\rangle$, $|q\bar{q}g\rangle$ produced at short-distance by a high momentum transfer process, follow by the Fock state binding to quarkonium process at long-distance. Where $|q\bar{q}\rangle$ has the same quantum numbers as its parent bound states in leading Fock state approximation.

Taking $B_c^- \rightarrow J/\Psi(\eta_c)\pi^-$ for example, all the non-perturbative binding effects are attributed to three parameters: pion decay constant and the Schrödinger wave functions at origin of $J/\Psi(\eta_c)$ and B_c . We express the detail in Appendix A, where the light-cone distribution amplitudes for light pseudoscalar and vector mesons, the NLO Schrödinger wave function at origin of J/Ψ determined by leptonic decay width and the non-relativistic projection operators for quarks hadronization in question are listed.

3.1 Tree-level results

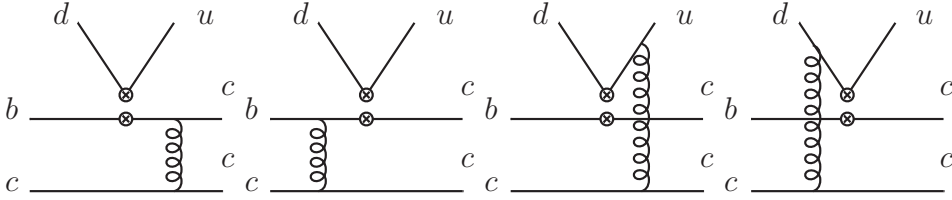


Figure 1: The quark-level Feynman diagrams in leading order for $B_c \rightarrow J/\Psi(\eta_c)\pi$. The 4-vertex “ $\otimes \otimes$ ” denotes the insertion of a 4-fermion operator Q_i . And the vivid figure in hadronic level is: B_c^+ annihilated to a pair of $\bar{b}c$ quarks; then strong and weak interactions appeared among quarks, followed by the annihilation of the \bar{b} quark and the creation of a \bar{c} and a pair of $u\bar{d}$ quarks; at last, $u\bar{d}$ bound to Pion while $c\bar{c}$ to S-Wave charmonium.

The possible quark-level topologies for $B_c \rightarrow J/\Psi(\eta_c)\pi$ are portrayed in Figure 1, where we assign momentum xP to the u -quark in the emitted pion with momentum P and momentum $(1-x)P$ to the d -quark. It is completely perturbatively calculable sector. The former two in Figure 1 contribute to $\langle Q_0 \rangle$, and the others contribute to $\langle Q_8 \rangle$. Associated with parameters belong to binding process: pion decay constant and the Schrödinger wave functions at origin of $J/\Psi(\eta_c)$ and B_c , we have the tree-level $\langle Q_i \rangle$, leaving the momentum fraction x unintegrated

$$\begin{aligned} \langle Q_0(\eta_c) \rangle_x &= \frac{8\sqrt{2}\pi f_\pi \psi_{\eta_c}(0) \psi_{B_c}(0) \phi_\pi(x) C_A C_F \alpha_s \sqrt{m_b + m_c} (m_b + 3m_c) (2m_b m_c + 3m_b^2 + 3m_c^2)}{m_c^{3/2} N_c (m_b - m_c)^3}, \\ \langle Q_8(\eta_c) \rangle_x &= \frac{2\sqrt{2}\pi f_\pi \psi_{\eta_c}(0) \psi_{B_c}(0) \phi_\pi(x) C_A C_F \alpha_s \sqrt{m_b + m_c} (m_b + 3m_c)^2 (xm_c - (x-1)m_b)}{m_c^{3/2} N_c^2 (m_c - m_b) ((x-1)m_b + (3x-2)m_c) (xm_b + (3x-1)m_c)}, \end{aligned} \quad (11)$$

where more detail about the long distance parameters f_π , $\psi_{\eta_c}(0)$ and $\psi_{B_c}(0)$ and pion light cone distribution amplitude $\phi_\pi(x)$ are expressed in Appendix A. Note that the $\langle Q_i \rangle$ vanishes for twist-3 distribution amplitude contribution of pion. Higher twist contribution comes from twist-4. And in a

similar way for J/Ψ , the corresponding matrix elements are

$$\begin{aligned}\langle Q_0(J/\Psi) \rangle_x &= -\frac{64\sqrt{2}\pi f_\pi \psi_{J/\Psi}(0) \psi_{B_c}(0) \phi_\pi(x) P_{B_c} \cdot \varepsilon_\Psi^* C_A C_F \alpha_s (m_b + m_c)^{5/2}}{m_c^{1/2} N_c (m_b - m_c)^4}, \\ \langle Q_8(J/\Psi) \rangle_x &= -\frac{8\sqrt{2}\pi f_\pi \psi_{J/\Psi}(0) \psi_{B_c}(0) \phi_\pi(x) P_{B_c} \cdot \varepsilon_\Psi^* C_A C_F \alpha_s (m_b + m_c)^{1/2}}{m_c^{1/2} N_c^2 (m_b - m_c)^2 ((x-1)m_b + (3x-2)m_c) (xm_b + (3x-1)m_c)} \\ &\quad \times (3(2x-1)m_b m_c + (x-1)m_b^2 + (9x-4)m_c^2). \end{aligned} \quad (12)$$

Note that $\langle Q_8 \rangle$ in Equation (11) and (12) is not symmetrical when exchange x with $1-x$, owing to the non-factorizable contribution from axial vector current in which the unintegrated amplitude has anti-symmetry after exchange x with $1-x$. However, those anti-symmetrical contribution can be easily proved to be zero after integrating the fraction x . We define the function $f(x)$ expressing the contribution from axial vector current, and then the above anti-symmetry indicates $f(1-x) = -f(x)$. Considering the pion LC distribution amplitude which is even symmetrical, i.e. $\phi_\pi(1-x) = \phi_\pi(x)$, we can get the results after integrating the fraction x

$$\int_0^1 f(x) \phi_\pi(x) dx = -\int_1^0 f(1-x) \phi_\pi(1-x) dx = -\int_0^1 f(x) \phi_\pi(x) dx = 0. \quad (13)$$

Employing asymptotic pion LCDA $\phi_\pi(x) = 6x\bar{x}$, we obtain the corresponding matrix elements $\langle Q_i \rangle$

$$\begin{aligned}\langle Q_0(\eta_c) \rangle &= \frac{8\sqrt{2}\pi f_\pi \psi_{\eta_c}(0) \psi_{B_c}(0) C_A C_F \alpha_s \sqrt{m_b + m_c} (m_b + 3m_c) (2m_b m_c + 3m_b^2 + 3m_c^2)}{m_c^{3/2} N_c (m_b - m_c)^3}, \\ \langle Q_8(\eta_c) \rangle &= \frac{6\sqrt{2}\pi f_\pi \psi_{\eta_c}(0) \psi_{B_c}(0) C_A C_F \alpha_s \sqrt{m_b + m_c}}{m_c^{3/2} N_c^2 (m_b - m_c) (m_b + 3m_c)} \times [2m_b m_c (\log(m_b + 2m_c) \\ &\quad - \log(m_c) + 2) + m_c^2 (4 \log(m_b + 2m_c) - 4 \log(m_c) + 3) + m_b^2], \\ \langle Q_0(\Psi) \rangle &= -\frac{64\sqrt{2}\pi f_\pi \psi_{J/\Psi}(0) \psi_{B_c}(0) P_{B_c} \cdot \varepsilon_\Psi^* C_A C_F \alpha_s (m_b + m_c)^{5/2}}{m_c^{1/2} N_c (m_b - m_c)^4}, \\ \langle Q_8(\Psi) \rangle &= -\frac{24\sqrt{2}\pi f_\pi \psi_{J/\Psi}(0) \psi_{B_c}(0) P_{B_c} \cdot \varepsilon_\Psi^* C_A C_F \alpha_s (m_b + m_c)^{1/2} \times [2m_b m_c (\log(m_b + 2m_c) \\ &\quad - \log(m_c) + 2) + m_c^2 (4 \log(m_b + 2m_c) - 4 \log(m_c) + 3) + m_b^2]}{m_c^{1/2} N_c^2 (m_b - m_c) (m_b + 3m_c)^3}. \end{aligned} \quad (14)$$

Apart from the traditional figure in which they factorize perturbatively hard kernel into matrix elements of the operators Q_i [12, 13], herein we extracted hard kernel T_i separately. They can be calculated order by order perturbatively.

$$\mathcal{A}(B_c^- \rightarrow J/\Psi(\eta_c) \pi^-) = \frac{G_F}{\sqrt{2}} V_{ud}^* V_{cb} (C_0(\mu) T_{f,0} M_f + C_0(\mu) T_{nf,0} M_{nf} + C_8(\mu) T_{nf,8} M_{nf}), \quad (15)$$

$$T_{f,i}(\mu) = \sum_{k=0}^{\infty} \left(\frac{\alpha_s}{4\pi}\right)^k T_{f,i}^{(k)}(\mu), \quad T_{nf,i}(\mu) = \sum_{k=0}^{\infty} \left(\frac{\alpha_s}{4\pi}\right)^k T_{nf,i}^{(k)}(\mu), \quad (16)$$

where T_f means factorizable hard kernel, T_{nf} means non-factorizable hard kernel. And the Wilson coefficients C_i are

$$C_0 = \frac{2}{3} C_+ + \frac{1}{3} C_-, \quad C_8 = C_+ - C_-, \quad (17)$$

where

$$C_\pm = \left[\frac{\alpha_s(M_W)}{\alpha_s(\mu)} \right]^{\frac{\gamma_\pm}{2\beta_0}}, \quad \gamma_\pm = \pm 6 \frac{N_c \mp 1}{N_c}, \quad \beta_0 = \frac{11N_c - 2n_f}{3}. \quad (18)$$

Considering the tree-level results as above and setting $M_f(\eta_c) = \langle Q_0(\eta_c) \rangle$, $M_f(J/\Psi) = \langle Q_0(\Psi) \rangle$, $M_{nf}(\eta_c) = \langle Q_8(\eta_c) \rangle$ and $M_{nf}(J/\Psi) = \langle Q_8(\Psi) \rangle$, we can extract the leading order hard kernel $T_i^{(0)}$ for charmonium

$$T_{f,0}^{(0)}(\eta_c) = T_{f,0}^{(0)}(J/\Psi) = 1, \quad T_{nf,0}^{(0)}(\eta_c) = T_{nf,0}^{(0)}(J/\Psi) = 0, \quad T_{nf,8}^{(0)}(\eta_c) = T_{nf,8}^{(0)}(J/\Psi) = 1. \quad (19)$$

3.2 One-loop results

Now we pay more attention to the corrections for the decay modes at next-to-leading order in the remainder of this section. The classified one loop diagrams for $B_c \rightarrow J/\Psi(\eta_c)\pi$ are shown in Figure 2, 3 and 4. Therein Figure 2 lays out the one loop factorizable diagrams while all of non-factorizable diagrams are collected in Figure 3 and 4. And we detailed some calculation techniques below. To regularize the Ultra-Violet and Infra-Red divergences we use dimensional regularization scheme, while relative velocity regularization scheme for Coulomb divergence. The renormalization constants are listed in Appendix B. In our calculation, the Mathematical package FeynArts [14] was used to generate the Feynman diagrams, FeynCalc [15] to deal with the amplitudes, and LoopTools [16] to calculate the one-loop integrals. The practicable γ_5 -scheme is adopted in D dimensional computation [17, 18].

3.2.1 $T_0^{(1)}$

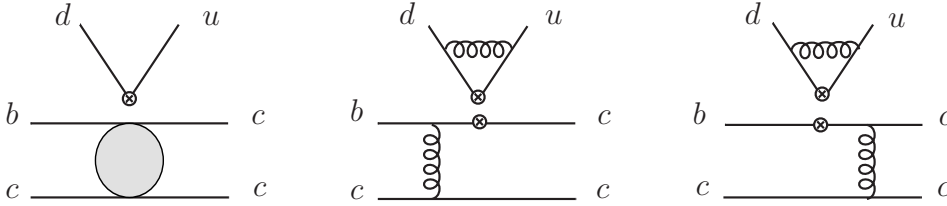


Figure 2: One loop factorizable diagrams contribute to $\langle Q_0 \rangle$. The bubble in the first diagram expresses all one loop form factor diagrams and explicit figures can be found in Ref. [21, 23].

The one loop diagrams contribute to $\langle Q_0 \rangle$ can be sorted into two kinds: factorizable (see Figure 2) and non-factorizable (see Figure 3). Further, we can employ the NLO B_c -to-S-wave-charmonium form factors which have been done in Ref. [21–24], and then obtain the contribution from the first figure in Figure 2 after convoluting the matrix element $\langle \pi | \bar{d}\gamma^\mu(1 - \gamma_5)u | 0 \rangle$ for the emission of pion. For the rear two of Figure 2, their UV divergence can be canceled by external field counter terms.

Note that the full analytic expression is too lengthy to presented, on the other hand it is possible to derive approximate analytic results valid in phenomenologically relevant research. Thus, we adopt the heavy quark limit, $m_b \rightarrow \infty$, in order to get analytic and approximate formulas.

At first, we analyzed the factorizable part. In the naive factorization (NF), $\langle Q_8 \rangle$ vanishes, and

$$\langle J/\psi(\eta_c)\pi^- | Q_0 | B_c^- \rangle \approx \langle J/\psi(\eta_c) | \bar{c}\gamma^\mu(1 - \gamma_5)b | B_c^- \rangle \langle \pi^- | \bar{d}\gamma_\mu(1 - \gamma_5)u | 0 \rangle, \quad (20)$$

i.e. $\langle Q_0 \rangle$ is proportional to the product of the pion decay constant and $B_c^- \rightarrow J/\psi(\eta_c)$ transition form-factor. Conventionally, we adopt the following parameterizations for the decay constants and

$B_c^- \rightarrow J/\psi(\eta_c)$ transition form-factors

$$\langle \eta_c(p) | \bar{c} \gamma_\mu \gamma_5 c | 0 \rangle = -i f_{\eta_c} p_\mu, \quad (21)$$

$$\langle \pi^-(p') | \bar{d} \gamma_\mu \gamma_5 u | 0 \rangle = -i f_\pi p'_\mu, \quad (22)$$

$$\langle B_c^-(P) | \bar{c} \gamma_\mu \gamma_5 b | 0 \rangle = -i f_{B_c} P_\mu, \quad (23)$$

$$\langle J/\psi(p, \varepsilon^*) | \bar{c} \gamma_\mu c | 0 \rangle = -i f_{J/\psi} m_{J/\psi} \varepsilon_\mu^*, \quad (24)$$

$$\langle \eta_c(p) | \bar{c} \gamma^\mu b | B_c^-(P) \rangle = f_+(q^2) \left[P^\mu + p^\mu - \frac{m_{B_c}^2 - m_{\eta_c}^2}{q^2} q^\mu \right] + f_0(q^2) \frac{m_{B_c}^2 - m_{\eta_c}^2}{q^2} q^\mu, \quad (25)$$

$$\langle \eta_c(p) | \bar{c} \gamma^\mu \gamma_5 b | B_c^-(P) \rangle = 0, \quad (26)$$

$$\langle J/\psi(p, \varepsilon^*) | \bar{c} \gamma^\mu b | B_c^-(P) \rangle = \frac{2iV(q^2)}{m_{B_c} + m_{J/\psi}} \epsilon^{\mu\nu\rho\sigma} \varepsilon_\nu^* p_\rho P_\sigma, \quad (27)$$

$$\begin{aligned} \langle J/\psi(p, \varepsilon^*) | \bar{c} \gamma^\mu \gamma_5 b | B_c^-(P) \rangle &= 2m_{J/\psi} A_0(q^2) \frac{\varepsilon^* \cdot q}{q^2} q^\mu + (m_{B_c} + m_{J/\psi}) A_1(q^2) \left[\varepsilon^{*\mu} - \frac{\varepsilon^* \cdot q}{q^2} q^\mu \right] \\ &\quad - A_2(q^2) \frac{\varepsilon^* \cdot q}{m_{B_c} + m_{J/\psi}} \left[P^\mu + p^\mu - \frac{m_{B_c}^2 - m_{J/\psi}^2}{q^2} q^\mu \right]. \end{aligned} \quad (28)$$

Here we define momentum transfer $q = P - p$ and $\epsilon^{0123} = -1$. Note that $f_0(0) = f_+(0)$.

The tree-level form factors can be calculated easily. They read

$$f_+^{LO}(q^2) = \frac{8\sqrt{2}C_A C_F \pi \sqrt{z+1} (-q^2 + 3z^2 + 2z + 3) \alpha_s \psi(0)_{B_c} \psi(0)_{\eta_c}}{(q^2 - (z-1)^2)^2 z^{3/2} m_b^3 N_c}, \quad (29)$$

$$f_0^{LO}(q^2) = \frac{8\sqrt{2}C_A C_F \pi \sqrt{z+1} (9z^3 + 9z^2 + 11z - q^2(5z+3) + 3) \alpha_s \psi(0)_{B_c} \psi(0)_{\eta_c}}{(q^2 - (z-1)^2)^2 z^{3/2} (3z+1) m_b^3 N_c}, \quad (30)$$

$$V^{LO}(q^2) = \frac{16\sqrt{2}C_A C_F \pi (3z+1) \alpha_s \psi(0)_{B_c} \psi(0)_{J/\Psi}}{(q^2 - (z-1)^2)^2 \left(\frac{z}{z+1}\right)^{3/2} m_b^3 N_c}, \quad (31)$$

$$A_0^{LO}(q^2) = \frac{16\sqrt{2}C_A C_F \pi (z+1)^{5/2} \alpha_s \psi(0)_{B_c} \psi(0)_{J/\Psi}}{(q^2 - (z-1)^2)^2 z^{3/2} m_b^3 N_c}, \quad (32)$$

$$A_1^{LO}(q^2) = \frac{16\sqrt{2}C_A C_F \pi \sqrt{z+1} (4z^3 + 5z^2 + 6z - q^2(2z+1) + 1) \alpha_s \psi(0)_{B_c} \psi(0)_{J/\Psi}}{(q^2 - (z-1)^2)^2 z^{3/2} (3z+1) m_b^3 N_c}, \quad (33)$$

$$A_2^{LO}(q^2) = \frac{16\sqrt{2}C_A C_F \pi \sqrt{z+1} (3z+1) \psi(0)_{B_c} \psi(0)_{J/\Psi}}{(q^2 - (z-1)^2)^2 z^{3/2} m_b^3 N_c}. \quad (34)$$

Here, $z \equiv m_c/m_b$.

Those form factors at next-to-leading order accuracy in heavy quark limit can be found in Ref. [21, 23].

Thus, in NF, neglecting the mass of pion, we have the factorizable contribution

$$\begin{aligned}\langle \eta_c \pi^- | Q_{0,f} | B_c^- \rangle &= i f_\pi f_0(0) (m_{B_c}^2 - m_{\eta_c}^2), \\ \langle J/\psi \pi^- | Q_{0,f} | B_c^- \rangle &= -i f_\pi A_0(0) (m_{B_c}^2 - m_{J/\psi}^2).\end{aligned}\quad (35)$$

Here we have used the fact that J/ψ is longitudinally polarized so that

$$2m_{J/\psi} \varepsilon^* \cdot P = 2m_{B_c} |\vec{p}_c| = m_{B_c}^2 - m_{J/\psi}^2.$$

And

$$\langle \eta_c \pi^- | Q_0 | B_c^- \rangle^{LO} = -i f_\pi f_{\eta_c}^{\text{NR}} f_{B_c}^{\text{NR}} \frac{4\pi\alpha_s C_F}{N_c} \frac{(1+z)(3+11z+9z^2+9z^3)}{z(1-z)^3}, \quad (36)$$

$z \rightarrow 0$ limit:

$$\lim_{z \rightarrow 0} \langle \eta_c \pi^- | Q_0 | B_c^- \rangle^{LO} = -i f_\pi f_{\eta_c}^{\text{NR}} f_{B_c}^{\text{NR}} \frac{4\pi\alpha_s C_F}{N_c} \frac{3}{z}. \quad (37)$$

However, in reality the above approximation is not so good. Numerically, we have

$$\left. \frac{\lim_{z \rightarrow 0} \langle \eta_c \pi^- | Q_0 | B_c^- \rangle^{LO}}{\langle \eta_c \pi^- | Q_0 | B_c^- \rangle^{LO}} \right|_{z=1.5/4.8} \approx 0.1, \quad (38)$$

which is essentially bad. The perturbative series expanded as (15) and (19), however, can resolve the problem. Where the expansion kernel according to m_c/m_b is the ratio of NLO result to LO one, and its convergence is well-behaved [24].

Obviously, the factorizable part of one loop hard kernel $T_{f,0}^{(1)}$ is proportional to the ratio of one loop form factor to the tree level form factor. Note that the analytic expression is too lengthy to presented, on the other hand it is possible to derive approximate analytic results valid in phenomenologically relevant research. Thus, we adopt the heavy quark limit, $m_b \rightarrow \infty$, in order to get analytic and approximate formulas. That is

$$\begin{aligned}T_{f,0}^{(1)}(\eta_c) = \frac{f_0^{(1)}(0)}{f_0^{(0)}(0)} &= \frac{1}{3}(11C_A - 2n_f) \ln\left(\frac{2\mu^2}{zm_b^2}\right) - \frac{10n_f}{9} - \frac{1}{3} \ln z - \frac{2 \ln 2}{3} \\ &+ C_F \left(\frac{1}{2} \ln^2 z + \frac{10}{3} \ln 2 \ln z - \frac{35}{6} \ln z + \frac{2 \ln^2 2}{3} \right. \\ &+ 3 \ln 2 + \frac{7\pi^2}{9} - \frac{103}{6} \Big) \\ &+ C_A \left(-\frac{1}{6} \ln^2 z - \frac{1}{3} \ln 2 \ln z - \frac{1}{3} \ln z + \frac{\ln^2 2}{3} \right. \\ &\left. - \frac{4 \ln 2}{3} - \frac{5\pi^2}{36} + \frac{73}{9} \right),\end{aligned}\quad (39)$$

$$\begin{aligned}T_{f,0}^{(1)}(\Psi) = \frac{A_0^{(1)}(0)}{A_0^{(0)}(0)} &= \frac{1}{3}(11C_A - 2n_f) \ln\left(\frac{2\mu^2}{zm_b^2}\right) - \frac{10n_f}{9} + C_F \left(\frac{1}{2} \ln^2 z - \frac{119}{8} \right. \\ &+ 7 \ln 2 \ln z - \frac{21}{4} \ln z + 7 \ln^2 2 + \frac{15 \ln 2}{4} \Big) \\ &+ C_A \left(-\frac{3}{8} \ln^2 z - \ln 2 \ln z - \frac{9}{8} \ln z - \frac{7\pi^2}{24} + \frac{67}{9} \right. \\ &\left. - \frac{9 \ln^2 2}{4} + \frac{3 \ln 2}{8} \right).\end{aligned}\quad (40)$$

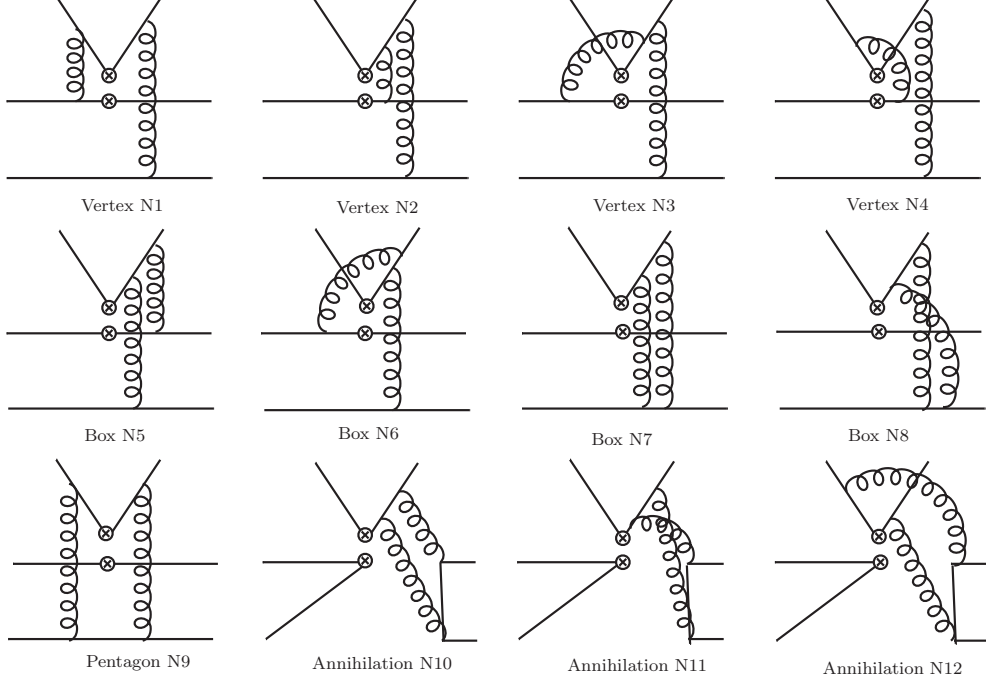


Figure 3: Travel of the twenty-four one loop non-factorizable diagrams contribute to $\langle Q_0 \rangle$. Another travel diagrams can be obtained by interchanging u and d quark.

Table 1: Color factors of the diagrams in Figure 3. Among them, the figures form N1 to N9, contribute not only to $\langle Q_0 \rangle$, but also to $\langle Q_8 \rangle$.

Diagram	N3-N5,N7	N1-N2,N6,N8-N9	N10-N12
color in $\langle Q_8 \rangle$	$-\frac{C_F}{2}$	$\frac{(C_A^2-2)C_F}{4}$	0
color in $\langle Q_0 \rangle$	$\frac{C_A C_F}{2}$		

Next, we concentrated on non-factorizable part. There are twenty-four one loop non-factorizable diagrams contribute to $\langle Q_0 \rangle$, half of which are displayed in Figure 3. Therein we tabbed them with a number. The corresponding color factors are summed up in Table 1. Around hundred of one-loop integrals in Figure 3 and Figure 4 can be reduced into a set of three-point, four-point scalar Passarino-Veltman integrals [16], plus some two-point integrals which can be easily calculated. Just considering the three-point and four-point integrals, we call them Master Integrals (MI). Wherein, the analytic formulas of infra-red and collinearly divergent scalar three-point and four-point integrals can be found in Ref. [25]. The analytic asymptotic form of master integrals are given out in Appendix C. Our analytic expressions of MI agreed with what given in Ref. [26] and were checked numerically by the package LoopTools.

In heavy quark limit, the analytical one loop non-factorizable matrix elements with momentum fraction x unintegrated can be found in Appendix D. After the fraction was integrated, the numerical one loop non-factorizable contribution for $T_{nf,0}^{(1)}$ are

$$T_{nf,0}^{(1)}(\eta_c) = 6 \log\left(\frac{m_b^2}{\mu^2}\right) + 16.75, \quad (41)$$

$$T_{nf,0}^{(1)}(\Psi) = T_{nf,0}^{(1)}(\eta_c). \quad (42)$$

And the complete results in heavy quark limit can be found in Appendix D.

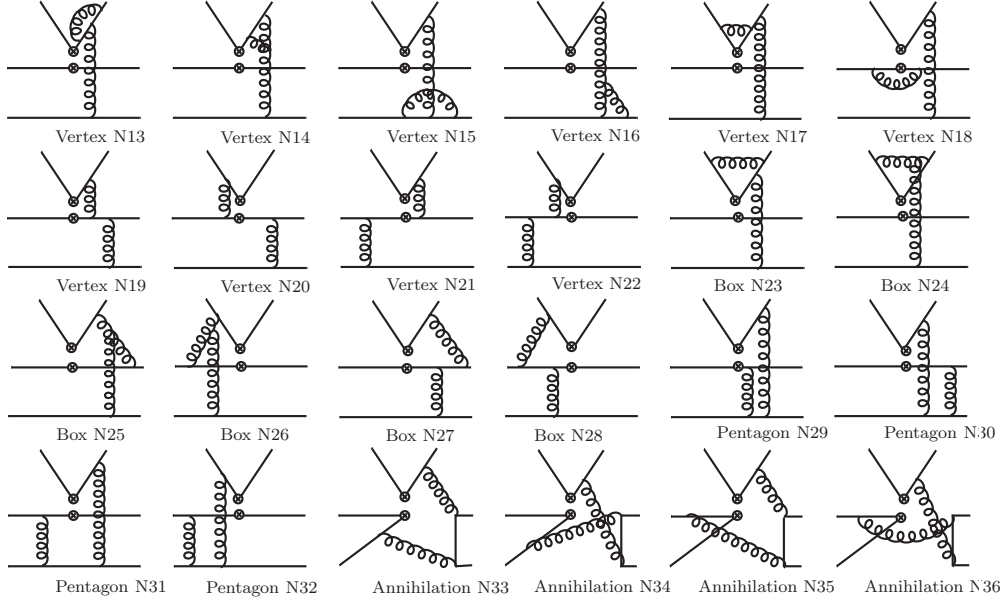


Figure 4: twenty-four of the sixty-five one loop non-factorizable diagrams contribute to $\langle Q_8 \rangle$. Another twenty-three diagrams can be obtained by interchanging u and d quark. In addition, the left eighteen comes from the diagrams Vertex N1 to Pentagon N9 in Figure 3 and their symmetrical partners.

Table 2: Color factors contribute to $\langle Q_8 \rangle$ of the diagrams in Figure 4.

Diagram	N14,N26	N16,N24-N25	N19-N23,N30-N32	N13,N15,N17-N18,N27-N29,N33-N36
color in $\langle Q_8 \rangle$	$\frac{iC_A^2 C_F}{4}$	$-\frac{iC_A^2 C_F}{4}$	$-\frac{C_A C_F}{12}$	$\frac{2C_A C_F}{3}$

3.2.2 $T_8^{(1)}$

Here, we study the one loop non-factorizable contributions to $\langle Q_8 \rangle$. Twenty-four diagrams are showed up in Figure 4, another nine diagrams are collected in Figure 3 form N1 to N9, and the rest can be obtained by interchanging u and d quarks. The corresponding color factors are summed up in Table 1 and Table 2.

The one loop contributions to $\langle Q_8 \rangle$ with momentum fraction x unintegrated in heavy quark limit can be found in Appendix D. After integrating the fraction, we have the corresponding $T_{nf,8}^{(1)}$ numerically

$$\begin{aligned}
T_{nf,8}^{(1)}(\eta_c) = & \frac{1}{3}(-11C_A + 2n_f + 16N_c - 6)\log\left(\frac{m_b^2}{\mu^2}\right) - \frac{12.48}{C_A} + (9\log z + 1)C_F \\
& - \left(\frac{\log^2 z}{2} - \frac{6\log 2 - 23}{3}\log z + 278.1\right)C_A - \frac{2}{9}n_f(-3\log z + 5 + 3\log 2) \\
& + \frac{\log^2 z}{6} - \frac{8(3 + \log 2)}{3}\log z + 548.9,
\end{aligned} \tag{43}$$

$$\begin{aligned}
T_{nf,8}^{(1)}(\Psi) = & \frac{1}{9}(-33C_A + 6n_f + 32N_c - 18)\log\left(\frac{m_b^2}{\mu^2}\right) - \frac{12.48}{C_A} + (9\log z + 1)C_F \\
& - \left(\frac{\log^2 z}{2} - \frac{6\log 2 - 23}{3}\log z + 278.1\right)C_A - \frac{2}{9}n_f(-3\log z + 5 + 3\log 2) \\
& + \frac{\log^2 z}{6} - \frac{8(3 + \log 2)}{3}\log z + 542.3.
\end{aligned} \tag{44}$$

4 The light-cone factorization scheme

Here we adopt Beneke and Jäger's version of the QCD factorization formula [27] rather than the version in the original BBNS paper [28, 29]. Here we take M_2 as the light meson emitted from the current-current interaction while the M_1 is the light meson recoils against B_c meson. Thus,

$$\begin{aligned} \langle M_1 M_2 | Q_i | \bar{B}_c \rangle = & im_{B_c}^2 \left\{ f_+^{BM_1}(0) \int_0^1 du T_{i,I}(u) f_{M_2} \phi_{M_2}(u) \right. \\ & \left. + \int_0^\infty d\omega \int_0^1 dudv T_{i,II}(\omega, u, v) \hat{f}_B \phi_{B_c+}(\omega) f_{M_1} \phi_{M_1}(v) f_{M_2} \phi_{M_2}(u) \right\}, \end{aligned} \quad (45)$$

and T_{II} can be further factorized into the following form

$$T_{i,II}(\omega, u, v) = -\frac{m_{B_c}}{8m_b} \int_0^1 d\tau H_{i,II}(u, \tau) J_{\parallel}(1 - \tau; v, \omega), \quad (46)$$

where $H_{i,II}$ and J_{\parallel} are perturbatively calculable hard-function and jet-function, respectively. Thus, the perturbative expansion of the matrix-elements of Q_i can be organized by the corresponding perturbatively calculable quantities defined above, namely $T_{i,I}$, $H_{i,II}$ and J_{\parallel} . We adopt the following convention for a perturbative quantity, say O ,

$$O = O^{(0)} + \frac{\alpha_s}{4\pi} O^{(1)} + \dots \quad (47)$$

$T_{i,I}$ has been calculated up to NNLO in α_s , $H_{i,II}$ and J_{\parallel} have been known at NLO in α_s in Soft Collinear Effective Theory (SCET). Since we are aimed to get NLO predictions for $B_c^- \rightarrow J/\psi(\eta_c)\pi^-$, we pile up the known results for the above quantities up to NLO.

4.1 Definition and matching

- T_I : At the tree-level, $T_{0,I}^{(0)}(u) = 1$ to reproduce the results of naive factorization, while $T_{8,I}^{(0)}(u) = 0$ for the vanishing trace of T^A . At the one-loop level, $T_{0,I}^{(1)}(u)$ vanishes also for the vanishing trace of T^A , and

$$\begin{aligned} T_{0,I}^{(0)}(u) &= 1, \\ T_{0,I}^{(1)}(u) &= 0, \\ T_{8,I}^{(0)}(u) &= 0, \\ T_{8,I}^{(1)}(u; \mu) &= \frac{C_F}{2N_c} V(u), \end{aligned} \quad (48)$$

with

$$\begin{aligned} V(u) = & -12 \ln \frac{\mu}{m_b} - 18 + 3 \left(\frac{1-2u}{\bar{u}} \ln u - i\pi \right) \\ & + \left\{ 2\text{Li}_2(u) - \ln^2 u + 2 \frac{2 \ln u}{\bar{u}} - (3 + 2i\pi) \ln u - (u \leftrightarrow \bar{u}) \right\}. \end{aligned} \quad (49)$$

- Jet function J_{\parallel} :

$$J_{\parallel}(\bar{\tau}; v, \omega) = -\frac{4\pi\alpha_s C_F}{N_c} \frac{1}{m_B \omega \bar{v}} \left[\delta(\bar{\tau} - \bar{v}) + \frac{\alpha_s}{4\pi} j_{\parallel}(\bar{\tau}; v, \omega) \right]. \quad (50)$$

- Hard-fuction $H_{i,II}$: in $Q_{1,2}$ basis,

$$\begin{aligned} H_{2,II}(u, v) &= \frac{2}{N_c} \left(\frac{1}{u} + \frac{\alpha_s}{4\pi} r_1(u, v) \right), \\ H_{1,II}(u, v) &= \frac{2}{N_c} \frac{\alpha_s}{4\pi} r_2(u, v). \end{aligned} \quad (51)$$

Transforming them into the singlet-octet basis, one has

$$H_{0,II}(u, v) = H_{1,II}(u, v), \quad (52)$$

$$H_{8,II}(u, v) = -\frac{1}{6}H_{1,II}(u, v) + \frac{1}{2}H_{2,II}(u, v). \quad (53)$$

In all, if we treat $J/\psi(\eta_c)$ as a light meson, the decay amplitude of $B_c^- \rightarrow J/\psi(\eta_c)\pi^-$ is written as

$$\begin{aligned} \mathcal{A}(B_c^- \rightarrow J/\psi(\eta_c)\pi^-) &= \langle J/\psi(\eta_c)\pi^- | H_{eff} | B_c^- \rangle \\ &= i \frac{G_F}{\sqrt{2}} V_{ud}^* V_{cb} f_{\pi} f_+^{B_c \rightarrow J/\psi(\eta_c)}(0) m_{B_c}^2 \alpha_1(B_c \rightarrow J/\psi(\eta_c)), \end{aligned} \quad (54)$$

with

$$\begin{aligned} \alpha_1(B_c \rightarrow J/\psi(\eta_c)) &= C_1 + \frac{C_2}{N_c} + \frac{C_2}{N_c} \frac{\alpha_s C_F}{4\pi} V(\pi) \\ &\quad + \frac{\pi \alpha_s C_F}{N_c^2} \frac{f_{J/\psi(\eta_c)} \hat{f}_{B_c}}{m_b f_+^{B_c \rightarrow J/\psi(\eta_c)}(0) \lambda_{B_c}} [C_2 h_1(J/\psi(\eta_c)\pi) + C_1 h_2(J/\psi(\eta_c)\pi)], \\ &= C_0 + \frac{C_8}{2N_c} \frac{\alpha_s C_F}{4\pi} V(\pi) \\ &\quad + \frac{\pi \alpha_s C_F}{N_c^2} \frac{f_{J/\psi(\eta_c)} \hat{f}_{B_c}}{m_b f_+^{B_c \rightarrow J/\psi(\eta_c)}(0) \lambda_{B_c}} [C_0 h_2(J/\psi(\eta_c)\pi) \\ &\quad + \frac{C_8}{2} \left(h_1(J/\psi(\eta_c)\pi) - \frac{h_2(J/\psi(\eta_c)\pi)}{N_c} \right)], \end{aligned} \quad (55)$$

where

$$V(\pi) = \int_0^1 du V(u) \phi_{\pi}(u), \quad (56)$$

$$h_1(J/\psi(\eta_c)\pi) = \bar{\Delta}_{J/\psi(\eta_c)} \bar{\Delta}_{\pi} + \frac{\alpha_s}{4\pi} [R_1(J/\psi(\eta_c)\pi) + \bar{\Delta}_{\pi} J(J/\psi(\eta_c))], \quad (57)$$

$$h_2(J/\psi(\eta_c)\pi) = \frac{\alpha_s}{4\pi} R_2(J/\psi(\eta_c)\pi), \quad (58)$$

$$R_i(J/\psi(\eta_c)\pi) = \int_0^1 du dv \phi_{J/\psi(\eta_c)}(v) \phi_{\pi}(u) \frac{r_i(u, v)}{\bar{v}}, \quad i = 1, 2, \quad (59)$$

$$J(J/\psi(\eta_c)) = \int_0^{\infty} \frac{d\omega}{\omega} \phi_{B_{c+}} \int_0^1 d\tau j_{\parallel}(\tau; v, \omega) = \lambda_{B_c}^{-1(1)} + J_{\parallel}(J/\psi(\eta_c)), \quad (60)$$

$$\frac{1}{\lambda_{B_c}} = \int_0^{\infty} \frac{d\omega}{\omega} \phi_{B_{c+}}(\omega), \quad (61)$$

$$\Delta_M \equiv \int_0^1 dx \frac{\phi_M(x)}{x}, \quad \bar{\Delta}_M \equiv \int_0^1 dx \frac{\phi_M(x)}{\bar{x}}. \quad (62)$$

For comparisons, here we rewrite the decay amplitude in terms of the matrix-elements of the effective operators $Q_{0,8}$,

$$\langle Q_0 \rangle = f_\pi f_0^{B_c \rightarrow J/\psi(\eta_c)}(0) m_B^2 + \frac{\pi \alpha_s C_F}{N_c^2 z} f_{J/\psi(\eta_c)} \hat{f}_{B_c} f_\pi h_2(J/\psi(\eta_c) \pi), \quad (63)$$

$$\begin{aligned} \langle Q_8 \rangle &= f_\pi f_0^{B_c \rightarrow J/\psi(\eta_c)}(0) m_B^2 \frac{\alpha_s}{4\pi} \frac{C_F}{2N_c} V(\pi) \\ &\quad + \frac{\pi \alpha_s C_F}{2N_c^2 z} f_{J/\psi(\eta_c)} \hat{f}_{B_c} f_\pi \left(h_1(J/\psi(\eta_c) \pi) - \frac{h_2(J/\psi(\eta_c) \pi)}{N_c} \right), \end{aligned} \quad (64)$$

For B and light-mesons, their LCDAs cannot be calculated within the perturbation theory. However, for the LCDAs for B_c^- and $J/\psi(\eta_c)$, as in Ref. [22, 30, 31], they can be refactorized into products of perturbative calculable distributions and the Schödinger wave functions at the origin.

- The $B_c^- \rightarrow J/\psi(\eta_c)$ form-factor at the maximum recoil is presented the above section.
- The re-factorization for $\phi_{c\bar{c}}(v)$ and $\phi_{b\bar{c}}(\omega)$:

$$\begin{aligned} \phi_{J/\psi(\eta_c)}(v, \mu) &= \delta(v - 1/2) + \frac{\alpha_s C_F}{4\pi} \phi_{J/\psi(\eta_c)}^{(1)}(v, \mu), \\ \phi_{B_c^+}(w, \mu) &= \delta(w - m_c) + \frac{\alpha_s C_F}{4\pi} \phi_{B_c^+}^{(1)}(w, \mu), \end{aligned} \quad (65)$$

with the NLO corrections

$$\begin{aligned} \phi_{J/\psi(\eta_c)}^{(1)} &= 4 \left\{ \left(\ln \frac{\mu^2}{m_\psi^2 (1/2 - v)^2} - 1 \right) \left[\left(1 + \frac{1}{1/2 - v} \right) v \theta(1/2 - v) + (v \leftrightarrow \bar{v}) \right] \right\}_+ \\ &\quad + 4 \left\{ \frac{v(1 - v)}{(1/2 - v)^2} \right\}_{++}, \end{aligned} \quad (66)$$

$$\begin{aligned} \frac{\phi_{B_c^+}^{(1)}}{w} &= 2 \left[\left(\ln \left[\frac{\mu^2}{(w - m)^2} \right] - 1 \right) \left(\frac{\theta(m - w)}{m(m - w)} + \frac{\theta(w - m)}{w(w - m)} \right) \right]_+ + 4 \left[\frac{\theta(2m - w)}{(w - m)^2} \right]_{++} \\ &\quad + \frac{4\theta(w - 2m)}{(w - m)^2} - \frac{\delta(w - m)}{m} \left(\frac{1}{2} \ln^2 \frac{\mu^2}{m^2} - \ln \frac{\mu^2}{m^2} + \frac{3\pi^2}{4} + 2 \right). \end{aligned} \quad (67)$$

- The decay constants matching from SCET to NRQCD:

$$\begin{aligned} \hat{f}_{B_c} &= f_{B_c}^{\text{NR}} \left[1 + \frac{\alpha_s C_F}{4\pi} \left(3 \ln \frac{\mu}{m_b} - 4 \right) \right], \\ f_{\eta_c} &= f_{\eta_c}^{\text{NR}} \left[1 + \frac{\alpha_s C_F}{4\pi} (-6) \right], \end{aligned} \quad (68)$$

$$f_{J/\psi\parallel} = f_{J/\psi}^{\text{NR}} \left[1 + \frac{\alpha_s C_F}{4\pi} (-8) \right], \quad (69)$$

$$f_{\eta_c}^{\text{NR}} = i \sqrt{\frac{2}{m_P}} \langle \eta_c(P) | \psi^\dagger \chi | 0 \rangle_{\text{NR}} = 2i \sqrt{\frac{N_c}{m_{\eta_c}}} \psi(0), \quad (70)$$

$$f_{J/\psi}^{\text{NR}} = i \sqrt{\frac{2}{m_V}} \langle J/\psi(P, \epsilon^*) | \psi^\dagger \vec{\epsilon} \cdot \vec{\sigma} \chi | 0 \rangle_{\text{NR}} = 2i \sqrt{\frac{N_c}{m_{J/\psi}}} \psi_{J/\psi}(0), \quad (71)$$

$$f_{B_c}^{\text{NR}} = i \sqrt{\frac{2}{m_{B_c}}} \langle B_c(P) | \psi^\dagger \chi | 0 \rangle_{\text{NR}} = 2i \sqrt{\frac{N_c}{m_{B_c}}} \psi_{B_c}(0), \quad (72)$$

4.2 The LC's results

Adopting the above definition, we got the below convoluton

$$\bar{\Delta}_\pi = 3, \quad \bar{\Delta}_{\eta_c}^{(0)} = 2, \quad \lambda_{B_c}^{-1(0)} = \frac{1}{m_c}, \quad V(\pi) = 6 \log\left(\frac{m_b^2}{\mu^2}\right) - \frac{37}{2}, \quad (73)$$

$$\bar{\Delta}_{\eta_c}^{(1)} = C_F(2(2 \log(2) - 3) \log\left(\frac{m_b^2}{\mu^2}\right) + 4(2 \log(2) - 3) \log(z) - \frac{2\pi^2}{3} + 12 + 4 \log(2)), \quad (74)$$

$$\lambda_{B_c}^{-1(1)} = \frac{C_F}{4m_c}(-2 \log^2\left(\frac{m_b^2}{\mu^2}\right) - 4(2 \log(z) + 1) \log\left(\frac{m_b^2}{\mu^2}\right) - 8 \log^2(z) - 8 \log(z) - 3\pi^2 + 8), \quad (75)$$

$$\begin{aligned} R_1(\eta_c \pi) = & \frac{3}{4}C_F(-4 \log^2\left(\frac{m_b^2}{\mu^2}\right) + 4(13 + 8 \log(2)) \log\left(\frac{m_b^2}{\mu^2}\right) + 7\zeta(3) + 2\pi^2 - 68 - 240 \log(2)) \\ & + \text{CA}(-6(3 + 2 \log(2)) \log\left(\frac{m_b^2}{\mu^2}\right) - \frac{63\zeta(3)}{8} - \frac{\pi^2}{2} + 3 + 126 \log(2)), \end{aligned} \quad (76)$$

$$\begin{aligned} R_2(\eta_c \pi) = & 18 \log\left(\frac{m_b^2}{\mu^2}\right) + \frac{3\text{Li}_3(\frac{1}{4})}{8} - \frac{3\text{Li}_3(-2)}{2} + \frac{3}{2}\text{Li}_2\left(\frac{1}{4}\right) \log(2) + 3\text{Li}_2(-2) \log(2) + \frac{21\zeta(3)}{16} \\ & - \frac{\pi^2}{2} - \frac{111}{2} + \frac{5 \log^3(2)}{2} - 12 \log^2(2) + \frac{1}{8}\pi^2 \log(2) + 18 \log(2), \end{aligned} \quad (77)$$

$$\begin{aligned} J_{||}(\eta_c) = & C_F(2 \log^2\left(\frac{m_b^2}{\mu^2}\right) + (4 \log(z) + 10 - 12 \log(2)) \log\left(\frac{m_b^2}{\mu^2}\right) + 2 \log^2(z) - 2(6 \log(2) - 5) \log(z) \\ & + \pi^2 - 26 + 6 \log^2(2)) - \frac{2}{9}\text{CA}(-3(6 \log(2) - 11) \log\left(\frac{m_b^2}{\mu^2}\right) - 3(6 \log(2) - 11) \log(z) \\ & + 3\pi^2 - 85 + 9 \log^2(2) + 3 \log(2)) - \frac{8}{9}n_f T_f(-3 \log\left(\frac{m_b^2}{\mu^2}\right) - 3 \log(z) + 5 + 3 \log(2)). \end{aligned} \quad (78)$$

where the analytic integration of the jet-function can be found in appendix B.1 of Ref. [32], and the first inverse moment of the LCDA of charmonium and B_c can be found in Ref. [22].

Thus

$$T_{nf,0}^{(1)}(\eta_c)_{LC} = \frac{1}{3}R_2(\eta_c \pi), \quad (79)$$

$$\begin{aligned} T_{nf,8}^{(1)}(\eta_c)_{LC} = & \frac{1}{6}(R_1(\eta_c \pi) - \frac{1}{N_c}R_2(\eta_c \pi) + (\bar{\Delta}_{\eta_c}^{(1)} + m_b \bar{\Delta}_{\eta_c}^{(0)} \lambda_{B_c}^{-1(1)} + J_{||}(\eta_c)) \bar{\Delta}_\pi) \\ & + C_F(2V(\pi) - \frac{3}{2} \log\left(\frac{m_b^2}{\mu^2}\right) - 10), \end{aligned} \quad (80)$$

Numerically

$$T_{nf,0}^{(1)}(\eta_c)_{LC} = 6 \log\left(\frac{m_b^2}{\mu^2}\right) - 16.85, \quad (81)$$

$$\begin{aligned} T_{nf,8}^{(1)}(\eta_c)_{LC} = & (-\frac{3}{N_c} + 18C_F + \frac{4}{3}(n_f T_f - 5\text{CA})) \log\left(\frac{m_b^2}{\mu^2}\right) - \frac{4}{9}n_f T_f(-3 \log(z) + 5 + 3 \log(2)) \\ & - C_F \log^2 z + \frac{1}{3}(\text{CA}(6 \log(2) - 11) - (9 + 6 \log(2))C_F) \log z \\ & + 18.10\text{CA} - 80.70C_F + \frac{8.43}{N_c}, \end{aligned} \quad (82)$$

4.3 Comparison with NR scheme

After the careful computation, we found that the LC results presented in (81) and (82) is somewhat different with the NR results presented in (41) and (43). This situation is different with the case in $B \rightarrow \pi\pi$, where the pure QCD calculation in Ref. [34] is in agreement with the SCET calculation in Ref. [27,33] in heavy quark limit. For hard spectator interaction, the formula in $B \rightarrow \pi\pi$ is expanded by Λ_{QCD}/m_b , similarly the formula in $B_c \rightarrow J/\Psi(\eta_c)\pi$ is expanded by m_c/m_b . The technique difference between the pure QCD and NRQCD before the expansion is that the author in Ref. [34] gives the light quark in B meson a momentum close to Λ_{QCD} scale and sets the mass of light quarks to zero, while we fix the mass of charm quark in B_c and charmonia to its physical region. This may be a cause of the inconsistency in heavy quark limit, and it needs further investigation.

Besides, the over-lap contribution should never be neglected. The LC scheme predicts that the non-factorizable parts for the processes B_c decays to S-wave charmonia along with a pion where the vector state is longitudinally polarized, are identical except a reverse sign in heavy quark limit, which is true at LO and be in agreement with NRQCD scheme. However, the symmetry breaks at NLO. Because of the overlap contribution, higher twist contributes the final results in m_c/m_b expansion. And the factorizable parts for the processes are not reversal even at LO.

The quarks hadronization projectors with NRQCD framework are

$$\Pi_{\eta_c} = i\sqrt{\frac{N_c}{8m_c}}\psi(0)_{\eta_c}(\not{p} + 2m_c)\gamma_5, \quad (83)$$

for η_c with momentum p ; and

$$\Pi_{J/\psi} = i\sqrt{\frac{N_c}{8m_c}}\psi(0)_{J/\psi}(\not{p} + 2m_c)\not{\epsilon}^*, \quad (84)$$

for J/ψ with momentum p and polarization vector ϵ . Following the convention, and set $\psi(0)_{\eta_c} = \psi(0)_{J/\psi}$ with the heavy-quark spin symmetry, the tree-level amplitudes in heavy quark limit is

$$\begin{aligned} \mathcal{A}^{LO}(B_c^- \rightarrow \eta_c \pi^-) &= \frac{24\pi G_F C_F V_{ud}^* V_{cb} f_\pi \alpha_s \psi(0)_{B_c} \psi(0)_{\eta_c}}{z^{3/2} m_b} (C_1 + \frac{C_2}{N_c}), \\ \mathcal{A}^{LO}(B_c^- \rightarrow J/\psi \pi^-) &= -\frac{16\pi G_F C_F V_{ud}^* V_{cb} f_\pi \alpha_s \psi(0)_{B_c} \psi(0)_{\eta_c}}{z^{3/2} m_b} (C_1 + \frac{C_2}{N_c}). \end{aligned} \quad (85)$$

Considering the LO twist in m_c/m_b expansion before the calculation. And the projectors in heavy quark limit are

$$\begin{aligned} \Pi'_{\eta_c} &= i\sqrt{\frac{N_c}{8m_c}}\psi_{\eta_c}(0)\not{p}\gamma_5, \\ \Pi'_{J/\psi} &= i\sqrt{\frac{N_c}{8m_c}}\psi_{J/\psi}(0)m_\psi\not{\epsilon}^*, \end{aligned} \quad (86)$$

and setting the mass of charm quark propagator to zero, the amplitudes is relevant

$$\begin{aligned} \mathcal{A}^{LO}(B_c^- \rightarrow \eta_c \pi^-) &= -\mathcal{A}^{LO}(B_c^- \rightarrow J/\psi \pi^-) \\ &= \frac{12\pi G_F C_F V_{ud}^* V_{cb} f_\pi \alpha_s \psi(0)_{B_c} \psi(0)_{\eta_c}}{z^{3/2} m_b} (C_1 + \frac{C_2}{N_c}), \end{aligned} \quad (87)$$

The inconsistency between (85) and (87) shows that the over-lap contributes the processes $B_c \rightarrow J/\Psi(\eta_c)\pi$, and can not be ignored.

5 The phenomenological studies

The decay width can be written as:

$$\Gamma(B_c \rightarrow J/\Psi(\eta_c)\pi) = \frac{|p|}{8\pi m_{B_c}^2} |A(B_c \rightarrow J/\Psi(\eta_c)\pi)|^2. \quad (88)$$

Here the final momentum $|p| = (m_{B_c}^2 - m_\Psi^2)/2m_{B_c}$ in the B_c meson rest frame, with the input parameters below [35]

$$\begin{aligned} m_c &= 1.4 \pm 0.1 \text{GeV}, \quad m_b = 4.9 \pm 0.1 \text{GeV}, \quad \Lambda_{QCD} = 100 \text{MeV}, \quad G_F = 1.16637 \times 10^{-5} \text{GeV}^{-2}, \\ |V_{ud}^* V_{cb}| &= A\lambda^2(1 - \lambda^2/2 - \lambda^4/8), \quad n_f = 3, \quad N_c = 3, \quad C_F = 4/3, \quad |V_{us}^*| = 0.2252, \\ |V_{cb}| &= 0.0406, \quad f_\pi = 130.4 \text{MeV}, \quad f_\rho = 216 \text{MeV}, \quad f_K = 156.1 \text{MeV}, \quad f_K^* = 220 \text{MeV}, \end{aligned}$$

where $A = 0.814$, $\lambda = 0.2257$. The NLO Schrödinger wave functions at the origin for J/ψ is determined through its leptonic decay width $\Gamma_{ee}^\psi = 5.55 \text{keV}$ [35], which gives $|\psi_\Psi^{NLO}(0)|^2 = 0.0801(\text{GeV})^3$ and a factor of 1.79 than LO Schrödinger wave functions at the origin $|\psi_\Psi^{LO}(0)|^2 = 0.0447(\text{GeV})^3$ (see Appendix A). For B_c , we shall fix its value to be: $|\psi_{B_c}(0)|^2 = 0.1307(\text{GeV})^3$, which is derived under the Buchmüller-Tye potential [36]. The one loop result for strong coupling constant is used, i.e.

$$\alpha_s(\mu) = \frac{4\pi}{(11 - \frac{2}{3}n_f) \log(\frac{\mu^2}{\Lambda_{QCD}^2})}.$$

Within the above input parameters, we can readily obtain the decay width of B_c decays to S-Wave charmonium and pion at NLO accuracy. In practise, the renormalization scale μ may run from $2m_c$ to m_b , and the μ dependence of branching ratio is shown in Figure 5. Therein, we plot both kinds of NLO results: one letting $m_c/m_b \rightarrow 0$ in heavy-quark-limit; the other fixing the ratio m_c/m_b to its physical value. The first one is valid in leading m_c/m_b , while the latter summed to all orders of m_c/m_b . It turned out the leading order approximation within m_c/m_b expansion, namely Asymptotic NLO result account for more than 85% of the NLO result. That means it is enough for us to use this analytic and simple expression for phenomenological studies in place of complicated NLO expression with Asymp. NLO result. The NLO corrections can reduce the uncertainty which is performed in Figure 6.

Moreover, we want to know how important the factorizable part is at NLO accuracy. After calculation, we found that the asymptotic factorizable contribution in heavy quark limit can be well-represented the majority for the branching ratio. At $m_c = 1.4 \text{GeV}$, $m_b = 4.9 \text{GeV}$ and $\mu = 3 \text{GeV}$, we obtain

$$\begin{aligned} Br(B_c \rightarrow \eta_c \pi)^{\text{Asymp. factorizable}} &= 5.10\%, \quad Br(B_c \rightarrow \eta_c \pi)^{\text{total}} = 5.20\%, \\ Br(B_c \rightarrow J/\Psi \pi)^{\text{Asymp. factorizable}} &= 3.06\%, \quad Br(B_c \rightarrow J/\Psi \pi)^{\text{total}} = 2.91\%. \end{aligned} \quad (89)$$

Apart from the uncertainty of renormalization scale, we also researched the uncertainty from quark mass. We found that both of them are the largest two theoretical uncertainties. The vivid figure of quark mass and renormalization scale dependence is drawn in Figure 7. In which, we also detailed the influences from Gegenbauer polynomials of light cone distribution amplitude of pion.

Considering the uncertainties stated above, we give our results in Table 3 for branching ratios of the B_c meson decays into S-Wave charmonium and light mesons and compare our results with that calculated from other models. The LO results are generally close to results of the QCD sum rule [37,38], the constituent quark model [39,43–45] and light-front ISGW model [40], however larger than results of the relativistic potential model [41] and the relativistic quark model [42]. Our work

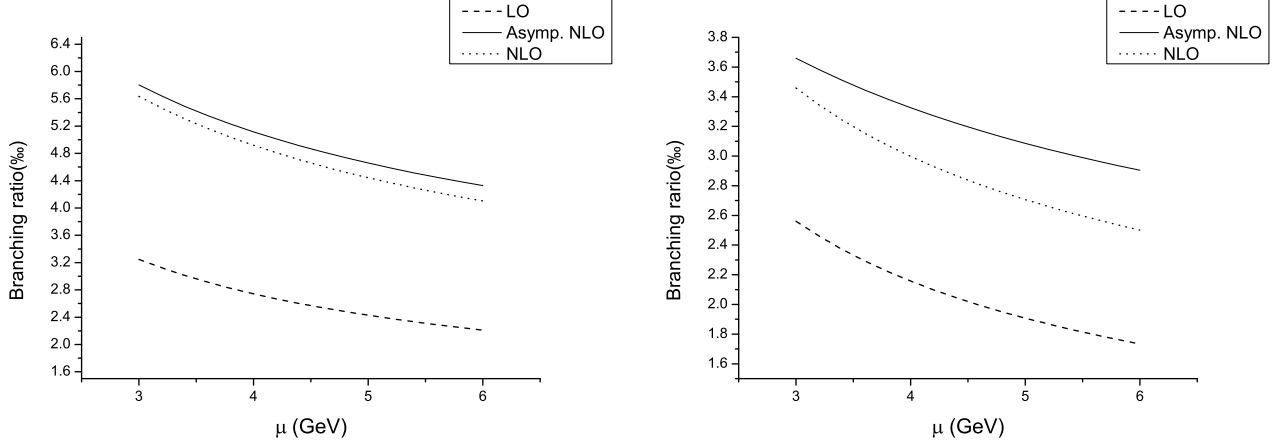


Figure 5: The branching ratios of $B_c \rightarrow \eta_c \pi$ (left) and $B_c \rightarrow J/\Psi \pi$ (right) versus renormalization scale μ . Herein $m_c = 1.5\text{GeV}$, $m_b = 4.8\text{GeV}$, and for the lifetime of the B_c we take $\tau(B_c) = 0.453\text{ ps}$. The results of LO accuracy, Asymptotic NLO one and complete NLO one are shown.

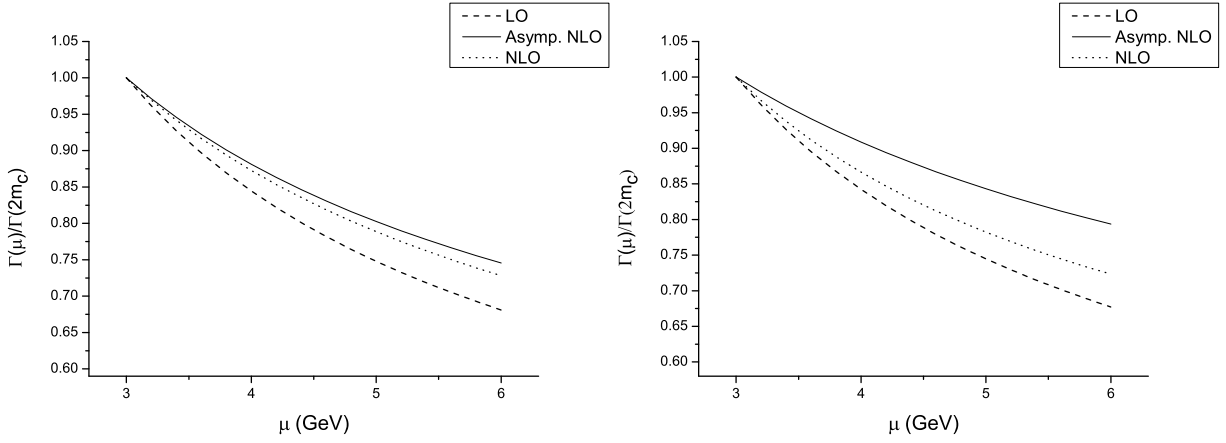


Figure 6: The ratio $\Gamma(\mu)/\Gamma(2m_c)$ of $B_c \rightarrow \eta_c \pi$ (left) and $B_c \rightarrow J/\Psi \pi$ (right) versus renormalization scale μ . Herein $m_c = 1.5\text{GeV}$, $m_b = 4.8\text{GeV}$. The μ dependence for LO, Asymptotic NLO and NLO are shown.

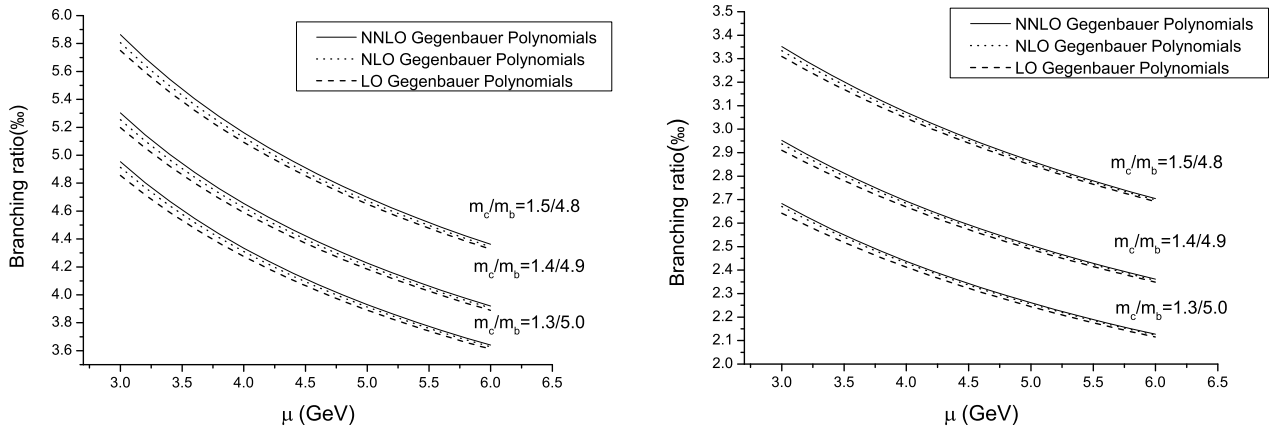


Figure 7: The branching ratio of $B_c \rightarrow \eta_c \pi$ (left) and $B_c \rightarrow J/\Psi \pi$ (right) versus renormalization scale μ , for different choices of quark mass. And LO, NLO, NNLO Gegenbauer polynomials of pion light cone distribution amplitude are shown.

Table 3: Branching ratios (in %) of exclusive non-leptonic B_c decays into ground state charmonium states. For the lifetime of the B_c we take $\tau(B_c) = 0.453$ ps. In our work, we chose the quantities $m_c = 1.4$ GeV, $m_b = 4.9$ GeV and $\mu = 3$ GeV. The uncertainty in the first column of the value is from varying the renormalization scale μ from 2.5 GeV to 5 GeV; while the uncertainty in the second column comes from varying the quark mass m_c/m_b from 1.5/4.8 to 1.3/5.0.

Mode	This work(NLO)	LO	[37,38]	[39]	[40]	[41]	[42]	[43]	[44]	[45]
$B_c^+ \rightarrow \eta_c \pi^+$	$5.19^{+0.44+0.55}_{-1.01-0.34}$	2.95	2.0	1.8	1.3	0.26	0.85	1.4	1.9	2.1
$B_c^+ \rightarrow \eta_c \rho^+$	$14.5^{+1.29+1.53}_{-2.92-0.95}$	7.89	4.2	4.9	3.0	0.67	2.0	3.3	4.5	-
$B_c^+ \rightarrow \eta_c K^+$	$0.38^{+0.03+0.04}_{-0.07-0.02}$	0.21	0.13	0.14	0.13	0.02	0.06	0.11	0.15	-
$B_c^+ \rightarrow \eta_c K^{*+}$	$0.77^{+0.07+0.08}_{-0.16-0.05}$	0.41	0.20	0.25	0.21	0.04	0.11	0.18	0.25	-
$B_c^+ \rightarrow J/\psi \pi^+$	$2.91^{+0.15+0.40}_{-0.42-0.27}$	2.22	1.3	1.8	0.73	1.3	0.61	1.1	1.7	1.9
$B_c^+ \rightarrow J/\psi \rho^+$	$8.08^{+0.45+1.09}_{-1.21-0.73}$	6.03	4.0	5.3	2.1	3.7	1.6	3.1	4.9	-
$B_c^+ \rightarrow J/\psi K^+$	$0.22^{+0.01+0.03}_{-0.03-0.02}$	0.16	0.11	0.14	0.07	0.07	0.05	0.08	0.13	-
$B_c^+ \rightarrow J/\psi K^{*+}$	$0.43^{+0.02+0.06}_{-0.07-0.04}$	0.32	0.22	0.29	0.16	0.20	0.10	0.18	0.28	-

Table 4: The events of $B_c \rightarrow J/\Psi \pi \rightarrow \mu^+ \mu^- \pi$, $B_c \rightarrow J/\Psi \pi \rightarrow e^+ e^- \pi$ and $B_c \rightarrow \eta_c \pi \rightarrow \gamma \gamma \pi$ with 10fb^{-1} data, using various values of the c -quark mass m_c and fixed b -quark mass $m_b = 4.8$ GeV.

-	Tevatron ($\sqrt{S} = 2$. TeV)					LHC ($\sqrt{S} = 14$. TeV)				
m_c (GeV)	1.4	1.5	1.6	1.7	1.8	1.4	1.5	1.6	1.7	1.8
σ_{B_c} (nb)	13.4	10.5	8.48	6.89	5.63	214	160	139	114	95.1
$\mu^+ \mu^- \pi$ ($\times 10^4$)	2.54	2.15	1.79	1.56	1.40	40.6	32.8	29.3	25.9	23.6
$e^+ e^- \pi$ ($\times 10^4$)	2.54	2.15	1.79	1.57	1.40	40.6	32.8	29.3	26.0	23.7
$\gamma \gamma \pi$	47	37	32	27	24	754	567	525	459	413

showed that the NLO corrections substantially enhance the branching ratios, and the NLO QCD correction K factors are, $1.75^{+0.14+0.18}_{-0.34-0.11}$ for $\Gamma(B_c \rightarrow \eta_c \pi)$ and $1.31^{+0.06+0.18}_{-0.18-0.12}$ for $\Gamma(B_c \rightarrow J/\Psi \pi)$.

Experimentally, the pp collisions at LHC have been performed at center-of-mass energy $\sqrt{s} = 8\text{TeV}$. And the energy will arrive at $\sqrt{s} = 14\text{TeV}$ in the future days. pp collisions provide a mass-production source for B_c meson. Since the B_c^* decays into the B_c with a probability of almost 100%, including the contributions from the S-wave excited states, the cross section of the B_c meson at LHC was estimated to be at a level of 10^2nb . With 10fb^{-1} of integrated luminosity, there are around 10^9 events for B_c production. Then, the measurements of $B_c \rightarrow J/\Psi \pi \rightarrow \mu^+ \mu^- \pi$ and $B_c \rightarrow J/\Psi \pi \rightarrow e^+ e^- \pi$ are feasible, and the events are presented in Table 4, in which we considered the quark mass dependence. Note that to obtain the prediction which includes complete the next-to-leading order of α_s , the NLO cross section of B_c hadronic production is needed. Here we employed the LO cross section of B_c hadronic production to predict the events. Even the lower branching ratio of $B(\eta_c \rightarrow \gamma \gamma) = (6.3 \pm 2.9) \times 10^{-5}$, there is of a potential to reconstruct the signal $B_c \rightarrow \eta_c \pi \rightarrow \gamma \gamma \pi$ as long as accumulating enough data at LHC region.

we also noticed that the LHCb collaboration have measured recently the ratio of branching fractions $Br(B_c^+ \rightarrow J/\Psi \pi^+ \pi^- \pi^+)/Br(B_c^+ \rightarrow J/\Psi \pi^+)$ to be $2.41 \pm 0.30 \pm 0.33$, using 0.8fb^{-1} data of pp collisions at center-of-mass energy $\sqrt{s} = 7\text{TeV}$ [8]. In which the constructed invariant mass distribution of the $\pi^+ \pi^- \pi^+$ combinations favors a resonance state $a_1^+(1260)$. So we also want to research the indirect ratio under the NRQCD framework and examine whether or not it can be used to explain the observation.

In theoretical aspects, there are mainly two channels $B_c^+ \rightarrow J/\Psi a_1^+(1260)$ followed with $a_1^+(1260) \rightarrow$

$\pi^+\pi^-\pi^+$ and $B_c^+ \rightarrow \Psi(2S)\pi^+$ with $\Psi(2S) \rightarrow J/\Psi\pi^+\pi^-$ which contribute to the signal of $B_c^+ \rightarrow J/\Psi\pi^+\pi^-\pi^+$. Practically, $Br(B_c^+ \rightarrow \Psi(2S)\pi^+)/Br(B_c^+ \rightarrow J/\Psi\pi^+) = (A_0^2(0)_\Psi(m_{B_c}^2 - m_{\Psi(2S)}^2)^3)/(A_0^2(0)_\Psi(m_{B_c}^2 - m_\Psi^2)^3) \approx 0.42$, and $Br(\Psi(2S) \rightarrow J/\Psi\pi^+\pi^-) = 33.6\%$ [35]. So the contribution to $Br(B_c^+ \rightarrow J/\Psi\pi^+\pi^-\pi^+)/Br(B_c^+ \rightarrow J/\Psi\pi^+)$ from $\Psi(2S)$ is 0.14, and it explained the experiment that favors the resonance state $a_1^+(1260)$ rather than $\Psi(2S)$.

We have did a complete QCD NLO calculation of B_c decays into S-wave charmonia and light mesons. And we found that the factorizable contribution account for more than 90% of total results at NLO accuracy in heavy quark limit as Eq. (89). Here we assume that it is also hold in $B_c^+ \rightarrow J/\Psi a_1^+(1260)$, i.e. it can reserve a high-accuracy just considering the factorizable diagrams. So we adopt the naive factorization scheme. And for the axial-vector meson $a_1^+(1260)$, the matrix element for its creation is

$$\langle a_1^+(1260)(p, \epsilon^*) | \bar{u}\gamma_\mu\gamma_5 d | 0 \rangle = -i f_{a_1} m_{a_1} \epsilon_\mu^*. \quad (90)$$

Then we can obtain the ratio

$$\frac{Br(B_c^+ \rightarrow J/\Psi a_1^+(1260))}{Br(B_c^+ \rightarrow J/\Psi\pi^+)} = \frac{f_{a_1}^2 \lambda_0}{f_\pi^2 A_0^2(0)} [\lambda_1 A_1^2(m_{a_1}^2) + \lambda_2 A_2^2(m_{a_1}^2) + \lambda_3 A_1(m_{a_1}^2) A_2(m_{a_1}^2) - \lambda_4 V^2(m_{a_1}^2)],$$

with

$$\lambda_0 = \frac{\sqrt{(m_{a_1}^2 + m_{B_c}^2 - m_\Psi^2)^2 - 4m_{a_1}^2 m_{B_c}^2}}{4m_\Psi^2 (m_{B_c} + m_\Psi)^2 (m_{B_c}^2 - m_\Psi^2)^3}, \quad (91)$$

$$\lambda_1 = (m_{B_c} + m_\Psi)^4 (-2m_{a_1}^2 (m_{B_c}^2 - 5m_\Psi^2) + m_{a_1}^4 + (m_{B_c}^2 - m_\Psi^2)^2), \quad (92)$$

$$\lambda_2 = (-2m_{a_1}^2 (m_{B_c}^2 + m_\Psi^2) + m_{a_1}^4 + (m_{B_c}^2 - m_\Psi^2)^2)^2, \quad (93)$$

$$\lambda_3 = 2(m_{B_c} + m_\Psi)^2 (m_{a_1}^2 - m_{B_c}^2 + m_\Psi^2) (m_{a_1}^2 - (m_{B_c} - m_\Psi)^2) (m_{a_1}^2 - (m_{B_c} + m_\Psi)^2), \quad (94)$$

$$\lambda_4 = -8m_{a_1}^2 m_\Psi^2 (-2m_{a_1}^2 (m_{B_c}^2 + m_\Psi^2) + m_{a_1}^4 + (m_{B_c}^2 - m_\Psi^2)^2). \quad (95)$$

Neglecting the isoscalar contributions to the two-pion state, we assume $Br(a_1^+(1260) \rightarrow \pi^+\pi^-\pi^+)$ is equal $Br(a_1^+(1260) \rightarrow \pi^+\pi^0\pi^0)$ and its value is 50% [46]. And we take the input parameters $f_{a_1} = 0.23\text{GeV}$ from the QCD sum rules [47], $m_{a_1} = 1.23\text{GeV}$ from the Particle Data Group [35]. The numerical results are

$$\frac{Br(B_c^+ \rightarrow J/\Psi\pi^+\pi^-\pi^+)}{Br(B_c^+ \rightarrow J/\Psi\pi^+)} = 2.75_{-0.04-0.05}^{+0.03+0.22},$$

The uncertainties of our result come from the renormalization scale and quark mass. It is compatible with the experimental data $2.41 \pm 0.30 \pm 0.33$ considering its uncertainty.

6 Conclusions

We have performed a comprehensive NLO analysis of the B_c decays into ground state charmonia and light mesons such as π , ρ , k and k^* . And in heavy quark limit, we also obtain the analytic formula of decay amplitude at NLO accuracy. And this simple expression can account for more than 85% of the complete NLO result in which fixing m_c/m_b to its physical value, therefor it is enough to use the formulas for phenomenological studies. The NLO QCD correction substantially enhance the results and reduce the μ dependence. The large branching ratio and the clear signal of the final states make it liable for the measurement of $B_c \rightarrow J/\Psi\pi$, $B_c \rightarrow J/\Psi\rho$ or $B_c \rightarrow J/\Psi K$ at the running LHC. Besides, in heavy quark limit, the consistence in this special case between with non-relativistic QCD scheme and with SCET is needed to be investigated furthermore.

Acknowledgement

This work was supported in part by the National Natural Science Foundation of China(NSFC) under the grants 10935012, 10821063 and 11175249.

Appendix

A Twist-2 and -3 LCDA for light pseudoscalar and vector mesons and non-relativistic projection operators for heavy quarkonia

Considering the twist-2 and twist-3 light-cone distribution amplitudes for pion, we have the matrix element in momentum space of quarks hadronization projection operator [13, 19]

$$\bar{u}_{\alpha a}(xP)\Gamma(x, \dots)_{\alpha\beta, ab, \dots} v_{\beta b}(\bar{x}P) \longrightarrow \frac{if_\pi}{4N_c} \int_0^1 dx M^\pi(x)_{\alpha\beta} \Gamma(x, \dots)_{\alpha\beta, aa, \dots}, \quad (96)$$

with the decay constant $f_\pi = 130.4\text{MeV}$, $\bar{x} = 1 - x$ and

$$M^\pi(x)_{\alpha\beta} = \left\{ \not{P}\gamma_5 \phi(x) - \mu_\pi \gamma_5 \left(\phi_p(x) - i\sigma_{\mu\nu} n_-^\mu v^\nu \frac{\phi'_\sigma(x)}{6} + i\sigma_{\mu\nu} P^\mu \frac{\phi_\sigma(x)}{6} \frac{\partial}{\partial k_{\perp\nu}} \right) \right\}_{\alpha\beta}, \quad (97)$$

here $\mu_\pi = m_\pi^2/(m_u + m_d)$, n_\pm are light cone vectors, $\phi(x)$ is twist-2 distribution amplitude and twist-3 one for $\phi_p(x)$ and $\phi_\sigma(x)$. For pion, up to twist-2 [13, 49]

$$\phi_\pi(x) = 6x\bar{x}\{1 + a_1 C_2^{3/2}(\bar{x} - x) + a_2 C_4^{3/2}(\bar{x} - x)\}, \quad (98)$$

with $a_1 = 0.44$, $a_2 = 0.25$, and the Gegenbauer polynomials are defined by

$$C_2^{3/2}(z) = \frac{3}{2}(5z^2 - 1), \quad C_4^{3/2}(z) = \frac{15}{8}(21z^4 - 14z^2 + 1). \quad (99)$$

Then, for vector meson ρ , the matrix element in momentum space of quarks hadronization projection operator is [13, 19]

$$\bar{u}_{\alpha a}(xP')\Gamma(x, \dots)_{\alpha\beta, ab, \dots} v_{\beta b}(\bar{x}P') \longrightarrow \frac{if_\rho}{4N_c} \int_0^1 dx M^\rho(x)_{\alpha\beta} \Gamma(x, \dots)_{\alpha\beta, aa, \dots}, \quad (100)$$

$$M_{\alpha\beta}^\rho = M_{\alpha\beta\parallel}^\rho + M_{\alpha\beta\perp}^\rho, \quad (101)$$

with

$$M_{\parallel}^\rho = -\frac{if_\rho}{4} \frac{m_\rho(\varepsilon^* \cdot n_+)}{2E} E \not{n}_- \phi_{\parallel}(u) - \frac{if_{\perp} m_\rho}{4} \frac{m_\rho(\varepsilon^* \cdot n_+)}{2E} \left\{ -\frac{i}{2} \sigma_{\mu\nu} n_-^\mu n_+^\nu h_{\parallel}^{(t)}(u) \right. \\ \left. - iE \int_0^u dv (\phi_{\perp}(v) - h_{\parallel}^{(t)}(v)) \sigma_{\mu\nu} n_-^\mu \frac{\partial}{\partial k_{\perp\nu}} + \frac{h_{\parallel}^{(s)}(u)}{2} \right\} \Big|_{k=up'}, \quad (102)$$

and

$$M_{\perp}^\rho = -\frac{if_{\perp}}{4} E \not{\varepsilon}_{\perp}^* \not{n}_- \phi_{\perp}(u) - \frac{if_{\rho} m_\rho}{4} \left\{ \not{\varepsilon}_{\perp}^* g_{\perp}^{(v)}(u) \right. \\ \left. - E \int_0^u dv (\phi_{\parallel}(v) - g_{\perp}^{(v)}(v)) \not{n}_- \varepsilon_{\perp\mu}^* \frac{\partial}{\partial k_{\perp\mu}} \right. \\ \left. + i\varepsilon_{\mu\nu\rho\sigma} \varepsilon_{\perp}^{*\nu} n_-^\rho \gamma^\mu \gamma_5 \left[n_+^\sigma \frac{g_{\perp}^{(a)}(u)}{8} - E \frac{g_{\perp}^{(a)}(u)}{4} \frac{\partial}{\partial k_{\perp\sigma}} \right] \right\} \Big|_{k=up'}. \quad (103)$$

Up to twist-2, the LCDA for longitudinally polarized ρ meson is

$$\phi_{\rho,\parallel}(x) = 6x\bar{x}\{1 + a_1^\rho C_2^{3/2}(\bar{x} - x)\}, \quad (104)$$

here $a_1^\rho = 0.18$.

In addition we used twist-2 LCDA for K meson [49]

$$\phi_K(x) = 6x\bar{x}\{1 + 0.51(\bar{x} - x) + 0.2C_2^{3/2}(\bar{x} - x)\}, \quad (105)$$

and that for longitudinally polarized K^* meson

$$\phi_{K^*,\parallel}(x) = 6x\bar{x}\{1 + 0.57(\bar{x} - x) + 0.07C_2^{3/2}(\bar{x} - x)\}, \quad (106)$$

At last, using leading Fock states for heavy quarkonium, the quarks hadronization projection operators are [18]

$$\begin{aligned} v(p_b) \bar{u}(p_c) &\rightarrow \frac{1}{2\sqrt{2}} \gamma_5 (\not{P}_{B_c} + m_b + m_c) \times \left(\frac{1}{\sqrt{\frac{m_b+m_c}{2}}} \psi_{B_c}(0) \right) \otimes \left(\frac{\mathbf{1}_c}{\sqrt{N_c}} \right), \\ v(p_{\bar{c}}) \bar{u}(p_c) &\rightarrow \frac{1}{2\sqrt{2}} \not{\epsilon} (\not{P}_\Psi + m_c + m_c) \times \left(\frac{1}{\sqrt{\frac{m_c+m_c}{2}}} \psi_\Psi(0) \right) \otimes \left(\frac{\mathbf{1}_c}{\sqrt{N_c}} \right). \end{aligned} \quad (107)$$

The NLO Schrödinger wave function at origin of J/Ψ determined by leptonic decay width is

$$|\psi_{J/\Psi}(0)|^2 = \frac{m_{J/\Psi}^2}{16\pi\alpha^2 e_c^2} \frac{\Gamma(J/\Psi \rightarrow e^+ e^-)}{(1 + \pi\alpha_s C_F/v - 4\alpha_s C_F/\pi)}. \quad (108)$$

B Renormalization and infre-red subtractions

The renormalization constants include Z_2 , Z_3 , Z_m , and Z_g , corresponding to heavy quark field, gluon field, quark mass, and strong coupling constant g , respectively. Here, in our calculation the Z_g is defined in the modified-minimal-subtraction ($\overline{\text{MS}}$) scheme, while for the other three the on-shell (OS) scheme is adopted, which tells

$$\begin{aligned} \delta Z_m^{OS} &= -3C_F \frac{\alpha_s}{4\pi} \left[\frac{1}{\epsilon_{UV}} - \gamma_E + \ln \frac{4\pi\mu^2}{m^2} + \frac{4}{3} + \mathcal{O}(\epsilon) \right], \\ \delta Z_2^{OS} &= -C_F \frac{\alpha_s}{4\pi} \left[\frac{1}{\epsilon_{UV}} + \frac{2}{\epsilon_{IR}} - 3\gamma_E + 3 \ln \frac{4\pi\mu^2}{m^2} + 4 + \mathcal{O}(\epsilon) \right], \\ \delta Z_3^{OS} &= \frac{\alpha_s}{4\pi} \left[(\beta_0 - 2C_A) \left(\frac{1}{\epsilon_{UV}} - \frac{1}{\epsilon_{IR}} \right) + \mathcal{O}(\epsilon) \right], \\ \delta Z_g^{\overline{\text{MS}}} &= -\frac{\beta_0}{2} \frac{\alpha_s}{4\pi} \left[\frac{1}{\epsilon_{UV}} - \gamma_E + \ln 4\pi + \mathcal{O}(\epsilon) \right]. \end{aligned} \quad (109)$$

While for light quark such as u and d quarks, the corresponding renormalization constant is

$$\delta Z_2^{OS} = -C_F \frac{\alpha_s}{4\pi} \left(\frac{1}{\epsilon_{UV}} - \frac{1}{\epsilon_{IR}} \right). \quad (110)$$

On above, $\delta Z_i = Z_i - 1$, and $\beta_0 = (11/3)C_A - (4/3)T_F n_f$ is the one-loop coefficient of the QCD beta function; $C_A = 3$ and $T_F = 1/2$ attribute to the $\text{SU}(3)$ group; μ is the renormalization scale.

We write the renormalized operator matrix elements as [21]

$$\langle Q_i \rangle_{\text{ren}} = Z_\psi \hat{Z}_{ij} \langle Q_j \rangle_{\text{bare}}, \quad (111)$$

where $i, j = 0, 8$ and $Z_\psi = Z_b^{1/2} Z_c^{1/2} Z_q$ contains the quark field renormalization factors of the massive b -quark Z_b , the massive c -quark Z_c and the massless quarks Z_q , whereas \hat{Z} is the operator renormalization matrix in the effective theory. It reads

$$\hat{Z} = 1 + \begin{pmatrix} 0 & 6 \\ \frac{4}{3} & -2 \end{pmatrix} \frac{\alpha_s}{4\pi} \frac{1}{\epsilon}. \quad (112)$$

All of soft IR divergences are canceled when sum them up, and then coulomb divergences can be canceled by the corresponding counter-term from the NLO Schrödinger wave function at origin. While the left collinear divergences can be removed by pion wave function subtraction [50].

C Master integrals

In this appendix we give a list of scalar triangle and box integrals that appear in the calculation. Other integrals can be obtained by interchanging x and $1-x$.

$$\text{C0}(p_1^2, p_2^2, (p_1 + p_2)^2, m_1^2, m_2^2, m_3^2) = \frac{(2\pi\mu)^{2\epsilon}}{i\pi^2} \int \frac{d^D q}{[q^2 - m_1^2][(q + p_1)^2 - m_2^2][(q + p_1 + p_2)^2 - m_3^2]}. \quad (113)$$

Herein, we use $D = 4 - 2\epsilon$ and μ is a scale introduced to keep the correct dimension of the integral in D space-time dimensions. We extract the leading order of the MI in $z = m_c/m_b$ expansion. Thus, all formulas below are valid up to order $\mathcal{O}(z)$. Therein, $\frac{1}{\epsilon} \equiv \frac{1}{\epsilon} - \gamma + \log(4\pi\mu^2)$ represents the infra-red pole. First, the integrals which have zero mass pole or m_c mass pole are

$$\begin{aligned} & \text{C0}\left(-\frac{m_c(m_b - m_c)^2}{2(m_b + m_c)}, 0, -\frac{(m_b - m_c)^2((x-1)m_b + (3x-2)m_c)}{2(m_b + m_c)}, 0, 0, 0\right) = \left[\frac{2\log(1-x) - 2\log(z)}{(x-1)m_b^2} \frac{1}{\epsilon} \right. \\ & \quad \left. + \frac{(\log(z) - \log(1-x))(2\log(m_b^2) + \log(z) - 2\log(2) + \log(1-x)) + \pi^2}{(x-1)m_b^2}\right], \\ & \text{C0}\left(\frac{(m_b - m_c)^2(m_b + 2m_c)}{2(m_b + m_c)}, 0, \frac{(m_b - m_c)^2(xm_b + (3x-1)m_c)}{2(m_b + m_c)}, 0, 0, 0\right) = \\ & \quad \left[-\frac{2\log(x)}{(x-1)m_b^2} \frac{1}{\epsilon} + \frac{\log(x)(2\log(m_b^2) + \log(x) - 2\log(2))}{(x-1)m_b^2}\right], \\ & \text{C0}\left(m_c^2, \frac{1}{2}(-2(x-1)m_b m_c - (x-1)m_b^2 + (3x-1)m_c^2), (m_b + m_c)^2 - x(m_b - m_c)(m_b + 3m_c), 0, m_c^2, 0\right) \\ & \quad = \left[-\frac{12\log(2)\log(z) + 6\log(2)\log(1-x) + \pi^2 - 9\log^2(2)}{3(x-1)m_b^2}\right], \\ & \text{C0}\left(m_c^2, -\frac{m_c((1-2x)m_b m_c - (x-1)m_b^2 + (3x-4)m_c^2)}{m_b + m_c}, -\frac{(m_b - m_c)^2((x-1)m_b + (3x-2)m_c)}{2(m_b + m_c)}, 0, m_c^2, 0\right) \\ & \quad = \left[\frac{6\log(2z)\log(1-x) - 3\log(z)(3\log(z) + 4\log(2)) + \pi^2 - 3\log^2(2)}{3(x-1)m_b^2}\right], \\ & \text{C0}\left(m_c^2, \frac{m_b((2x-1)m_b m_c + xm_b^2 - 3(x-1)m_c^2)}{m_b + m_c}, \frac{(m_b - m_c)^2(xm_b + (3x-1)m_c)}{2(m_b + m_c)}, 0, m_c^2, 0\right) \\ & \quad = \left[\frac{-12\log(2)\log(z) + 6\log(2)\log(x) + \pi^2 - 3\log^2(2)}{3xm_b^2}\right], \\ & \text{C0}\left(-\frac{m_b m_c(m_b - 3m_c)}{m_b + m_c}, 0, m_b\left(m_b - \frac{x(m_b - m_c)(m_b + 3m_c)}{m_b + m_c}\right), m_c^2, 0, 0\right) = \left[-\frac{\log(z) - \log(x-1)}{(x-1)m_b^2} \frac{1}{\epsilon} \right. \\ & \quad \left. - \frac{2\log(m_c^2)(\log(z) - \log(x-1)) - 4\log(z)\log(x-1) + 3\log^2(z) + \log^2(x-1)}{2(x-1)m_b^2}\right], \\ & \text{C0}\left(m_c^2, 0, -\frac{m_c((1-2x)m_b m_c - (x-1)m_b^2 + (3x-4)m_c^2)}{m_b + m_c}, m_c^2, 0, 0\right) = \left[\frac{1}{2(x-1)m_b m_c} \frac{1}{\epsilon^2} \right. \\ & \quad \left. + \frac{-\log(m_c^2) + 2\log(z) - 2\log(1-x)}{2(x-1)m_b m_c} \frac{1}{\epsilon} - \frac{\log(m_c^2)(\log(z) - \log(1-x))}{(x-1)m_b m_c} \right. \\ & \quad \left. + \frac{3\log^2(m_c^2) - 12\log(z)\log(1-x) + 6\log^2(z) + 6\log^2(1-x) - \pi^2}{12(x-1)m_b m_c}\right], \\ & \text{C0}\left(m_c^2, -\frac{m_b m_c(m_b - 3m_c)}{m_b + m_c}, -\frac{m_c(m_b - m_c)^2}{2(m_b + m_c)}, 0, m_c^2, 0\right) = \frac{6\log(2)\log(z) - \pi^2 + 3\log^2(2)}{3m_b m_c}, \\ & \text{C0}\left(m_c^2, m_c^2, -\frac{m_c(m_b - m_c)^2}{2(m_b + m_c)}, 0, m_c^2, 0\right) = -\frac{\log(z)(3\log(z) + 6\log(2)) + 4\pi^2 + 3\log^2(2)}{3m_b m_c}. \end{aligned} \quad (114)$$

In the following, the integrals are related to m_b poles

$$\begin{aligned}
& \text{C0} \left(m_b^2, 0, \frac{m_b ((2x-1)m_b m_c + x m_b^2 - 3(x-1)m_c^2)}{m_b + m_c}, m_b^2, 0, 0 \right) \\
&= \left[\frac{1}{2(x-1)m_b^2} \frac{1}{\epsilon^2} - \frac{\log(m_b^2) + 2\log(1-x)}{2m_b^2(x-1)} \frac{1}{\epsilon} \right. \\
&\quad \left. + \frac{12\log(1-x)\log(m_b^2) + 3\log^2(m_b^2) - 12\text{Li}_2\left(\frac{x}{x-1}\right) + 6\log^2(1-x) + \pi^2}{12(x-1)m_b^2} \right]. \\
& \text{C0} \left(m_b^2, m_c \left(\frac{x(m_c - m_b)(m_b + 3m_c)}{m_b + m_c} + m_c \right), (m_b + m_c)^2 - x(m_b - m_c)(m_b + 3m_c), 0, m_b^2, 0 \right) \\
&= -\frac{\text{Li}_2(x) + \text{Li}_2\left(\frac{x}{x-1}\right) + \log^2(1-x)}{x m_b^2}, \\
& \text{C0} \left(4m_c^2, \frac{m_c(-m_b m_c - m_b^2 + 4m_c^2)}{m_b + m_c}, m_b^2, 0, 0, m_b^2 \right) = -\frac{2\log^2(2z)}{m_b^2}. \tag{115}
\end{aligned}$$

Relating two kinds of mass are

$$\begin{aligned}
& \text{C0} \left(-\frac{m_c(m_b - m_c)^2}{2(m_b + m_c)}, \frac{1}{2}(-2(x-1)m_b m_c - (x-1)m_b^2 + (3x-1)m_c^2), m_b \left(m_b - \frac{x(m_b - m_c)(m_b + 3m_c)}{m_b + m_c} \right), \right. \\
& m_b^2, m_b^2, 0) = \frac{2(-\text{Li}_2(x) + \text{Li}_2\left(\frac{x+1}{2}\right) + \log(-x-1)\log\left(\frac{1-x}{2}\right) - \log(1-x)\log(-2x) + \log^2(2))}{(x-1)m_b^2}, \\
& \text{C0} \left(-\frac{m_c(m_b - m_c)^2}{2(m_b + m_c)}, \frac{1}{2}(-2(x-1)m_b m_c - (x-1)m_b^2 + (3x-1)m_c^2), m_b \left(m_b - \frac{x(m_b - m_c)(m_b + 3m_c)}{m_b + m_c} \right), \right. \\
& m_c^2, m_c^2, 0) = -\frac{6\log(2)(\log(1-x) - \log(z)) + \pi^2}{3(x-1)m_b^2}, \\
& \text{C0} \left(4m_c^2, -\frac{m_c((1-2x)m_b m_c - (x-1)m_b^2 + (3x-4)m_c^2)}{m_b + m_c}, m_b \left(m_b - \frac{x(m_b - m_c)(m_b + 3m_c)}{m_b + m_c} \right), m_c^2, m_c^2, 0 \right) \\
&= \frac{\log(z)(2\log(1-x) - 3\log(z))}{2(x-1)m_b^2}, \\
& \text{C0} \left(m_c^2, -\frac{m_b m_c(m_b - 3m_c)}{m_b + m_c}, -\frac{m_c(m_b - m_c)^2}{2(m_b + m_c)}, m_c^2, 0, m_c^2 \right) = -\frac{-6\log(2)\log(z) + \pi^2 - 9\log^2(2)}{3m_b m_c}, \\
& \text{C0} \left(m_c^2, \frac{m_c(-m_b m_c - m_b^2 + 4m_c^2)}{m_b + m_c}, \frac{(m_b - m_c)^2(m_b + 2m_c)}{2(m_b + m_c)}, m_c^2, 0, m_b^2 \right) \\
&= -\frac{12\text{Li}_2(-z) - 24\log(2)\log(z) + \pi^2 - 18\log^2(2)}{6m_b^2}, \\
& \text{C0} \left(m_c^2, m_c^2, -\frac{m_c(m_b - m_c)^2}{2(m_b + m_c)}, m_c^2, 0, m_c^2 \right) = \left[-\frac{6\log(z) + 6\log(2)}{3m_b m_c} \frac{1}{\epsilon} \right. \\
&\quad \left. + \frac{6\log(2z)\log(m_c^2) - 3\log(z)\log(4z) + \pi^2 - 3\log^2(2)}{3m_b m_c} \right], \\
& \text{C0} \left(m_c^2, 4m_c^2, -\frac{m_b m_c(m_b - 3m_c)}{m_b + m_c}, 0, m_c^2, m_c^2 \right) = -\frac{3\log^2(z) + 5\pi^2}{6m_b m_c}, \\
& \text{C0} \left(m_b^2, m_c^2, (m_b + m_c)^2, m_b^2, 0, m_c^2 \right) = -\frac{1}{2m_b m_c} \frac{1}{\epsilon} + \frac{\log(m_c^2) + 2}{2m_b m_c},
\end{aligned}$$

$$C0(m_c^2, m_c^2, 4m_c^2, m_c^2, 0, m_c^2) = -\frac{1}{2m_c^2} \frac{1}{\epsilon} + \frac{\log(m_c^2) + 2}{2m_c^2}. \quad (116)$$

Next, four box integrals are below

$$\begin{aligned} D0(m_b^2, m_c^2, \frac{1}{2}(-2(x-1)m_b m_c - (x-1)m_b^2 + (3x-1)m_c^2), m_c(xm_b + (1 - \frac{3x}{2})m_c) + \frac{xm_b^2}{2}, \\ (m_b + m_c)^2, -\frac{(m_b - m_c)^2((x-1)m_b + (3x-2)m_c)}{2(m_b + m_c)}, m_b^2, 0, m_c^2, 0) \\ = \frac{1}{(x-1)m_b^3 m_c} \frac{1}{\epsilon} - \frac{\log(m_c^2) + 2}{(x-1)m_b^3 m_c}, \\ D0(m_c^2, m_c^2, -\frac{m_c((1-2x)m_b m_c - (x-1)m_b^2 + (3x-4)m_c^2)}{m_b + m_c}, m_b(m_b - \frac{x(m_b - m_c)(m_b + 3m_c)}{m_b + m_c}), \\ 4m_c^2, -\frac{(m_b - m_c)^2((x-1)m_b + (3x-2)m_c)}{2(m_b + m_c)}, m_c^2, 0, m_c^2, 0) \\ = \frac{1}{(x-1)m_b^2 m_c^2} \frac{1}{\epsilon} + \frac{-\log(m_c^2) - 2 + 2\log(2)}{(x-1)m_b^2 m_c^2}, \\ D0(m_b^2, m_c^2, m_c^2, \frac{1}{2}(2m_b m_c + m_b^2 - m_c^2), (m_b + m_c)^2, -\frac{m_c(m_b - m_c)^2}{2(m_b + m_c)}, m_b^2, 0, m_c^2, 0) \\ = \frac{1}{m_b^2 m_c^2} \frac{1}{\epsilon} - \frac{\log(m_c^2) + 2}{m_b^2 m_c^2}, \\ D0(m_c^2, m_c^2, m_c^2, -\frac{m_b m_c(m_b - 3m_c)}{m_b + m_c}, 4m_c^2, -\frac{m_c(m_b - m_c)^2}{2(m_b + m_c)}, m_c^2, 0, m_c^2, 0) \\ = \frac{1}{m_b m_c^3} \frac{1}{\epsilon} - \frac{\log(m_c^2) - 2\log(2) + 2}{m_b m_c^3}. \end{aligned} \quad (117)$$

D Formulas for contributions of non-factorizable diagrams

In this subsection, the asymptotic formulas of one loop non-factorizable diagrams contributions with momentum fraction x unintegrated are expressed. They are valid in heavy quark limit. Besides, the complete results after integrating the light cone distribution amplitude of pion are also listed.

$$\begin{aligned} T_{\text{nf},0,x}^{(1)}(\eta_c) = \phi_\pi(x) \{ \frac{2}{x} \log(\frac{m_b^2}{\mu^2}) + \frac{2(x-1)\log^2(x)}{3x(2x-1)} - \frac{2(\text{Li}_2(\frac{x-1}{x}) - \text{Li}_2(\frac{x}{x-1}))}{3x} \\ - \frac{1}{3(x-1)x(2x-1)} f_1 - \frac{1}{3x(2x-1)} f_2 + \frac{1}{3(2x-1)^3} f_3 + \frac{1}{3(x-1)x(2x-1)^3} f_4 \\ + \frac{1}{3x^2(2x-1)^3} f_5 + \frac{1}{3(x-1)x^2(2x-1)^3} f_6 \}, \end{aligned} \quad (118)$$

$$T_{\text{nf},0,x}^{(1)}(\Psi) = T_{\text{nf},0,x}^{(1)}(\eta_c), \quad (119)$$

with

$$\begin{aligned} f_1 &= 2(x^2(\log(2) - 4) - x(2 + 2\log(2)) + 2 + \log(2)) \log(x+1), \\ f_2 &= 2(x-1)(-\text{Li}_2(\frac{x+1}{2x^2}) + \text{Li}_2(-\frac{1}{2x}) + 2\text{Li}_2(\frac{1}{x}) - \text{Li}_2(-2x) + \text{Li}_2(2(x+1))), \\ f_3 &= 8(x-1)^2(\text{Li}_2(4-2x) + 2\text{Li}_2(\frac{1}{1-x}) - \text{Li}_2(-\frac{x-2}{2(x-1)^2}) + \text{Li}_2(\frac{1}{2(x-1)}) - \text{Li}_2(2x-2)), \\ f_4 &= \log(x)(-4(2x^2 - 3x + 1)^2 \log(x+1) - 8x(x-1)^3 \log(2-x) + 3 + 6\log(2) \\ &\quad + x(2x(2x(-2x + 2(5x-14)\log(2) - 3) + 15 + 56\log(2)) - 17 - 46\log(2))), \\ f_5 &= \log(1-x)(x(4x(x-10x\log(2) + 5 + 18\log(2)) - 37 - 38\log(2)) + 19 + 4\log(2)) \\ &\quad + 2(x-1)x(\log(x+1) + 4(x-1)x(2\log(2-x) + \log(x+1))) - 3), \end{aligned}$$

$$\begin{aligned}
f_6 = & -8x^2(x-1)^3 \log^2(1-x) + (x-1)(x(x^2(20+8\log(2)) - x(72+16\log(2)) \\
& + 79+8\log(2)) - 32) + 4) \log(2-x) + x(2x(2x(28x^2-58x+45) - 31) \\
& + \pi^2(x-1)^2 + x(103-2x(6x(6x-13)+83)) \log(2) + 8-33\log(2)) + 4\log(2).
\end{aligned}$$

$$\begin{aligned}
T_{8,nf,x}^{(1)}(\eta_c) = & \phi_\pi(x) \left\{ \frac{-11C_A + 48xN_c + 2n_f - 6}{9x} \log\left(\frac{m_b^2}{\mu^2}\right) + \frac{9(x-1)\log(z) - 5x + 2}{3(x-1)x} C_F - \frac{(3C_A - 1)\log^2(z)}{18x} \right. \\
& - \frac{2(-3\log(z) + 5 + 3\log(2))}{27x} n_f - \frac{\log(z)}{54(x-1)x} ((138x - 144x\log(2) - 138 + 90\log(2))C_A + 144x \\
& + 96x^2\log(1-x) - 96x^2\log(x) - 96x\log(1-x) + 96x\log(x) + 372x\log(2) - 144 - 210\log(2)) \\
& + \frac{1}{C_A} \left(\frac{2(\text{Li}_2(\frac{x-1}{x}) - \text{Li}_2(\frac{x}{x-1}))}{3x} - \frac{(x-2)(x(10x-11)+2)\log(1-\frac{x}{2})}{3(1-2x)^2x^2} \right. \\
& + \frac{1}{3x(2x-1)} f_2 - \frac{1}{3(2x-1)^3} f_3 + \frac{1}{3(x-1)x(2x-1)^3} f_7 + \frac{1}{3x^2(2x-1)^3} f_8 + \frac{1}{3(x-1)x(2x-1)^3} f_9 \\
& + C_A \left(-\frac{(2x+1)(\text{Li}_2(\frac{x-1}{x}) - \text{Li}_2(\frac{x}{x-1}))}{3x} - \frac{(x^2\text{Li}_2(\frac{1-x}{2}) - x^2\text{Li}_2(\frac{x}{2}) + 2x\text{Li}_2(\frac{x}{2}) - \text{Li}_2(\frac{1-x}{2}))}{(x-1)x} + \frac{1}{6x} f_2 \right. \\
& - \frac{x-1}{3(2x-1)^3} f_3 + \frac{(-4x^2+x-1)\log(x)\log(2x+1)}{3x(2x-1)} - \frac{(x-2)(3x-2)(8x^2-6x+3)C_A\log(1-\frac{x}{2})}{6(1-2x)^2(x-1)x} \\
& + \frac{\log(x)}{6(x-1)x(2x-1)^3} f_{10} + \frac{\log(1-x)}{6x^2(2x-1)^3} f_{11} - \frac{1}{6(x-1)x^2(2x-1)^3} f_{12} + \frac{1}{108(x-1)x^2(2x-1)^3} f_{13} \\
& - \frac{(x^2-x+2)(\text{Li}_2(1-x) - \text{Li}_2(1-\frac{x}{2}))}{9(x-1)x} + \frac{(x-3)(\text{Li}_2(x) - \text{Li}_2(\frac{x+1}{2}))}{9x} - \frac{3(x-2)\text{Li}_2(\frac{x}{2})}{x-1} \\
& - \frac{7}{3}(\text{Li}_2(\frac{x-1}{x}) - \text{Li}_2(\frac{x}{x-1})) + \frac{3(x+1)\text{Li}_2(\frac{1-x}{2})}{x} + \frac{(x-2)(78x^2-51x-2)\log(1-\frac{x}{2})}{18(x-1)x^2} \\
& \left. + \frac{\log(x)}{18(x-1)x} f_{14} + \frac{\log(1-x)}{9(x-1)x^2} f_{15} + \frac{6}{108(x-1)x} f_{16} \right\}, \tag{120}
\end{aligned}$$

$$\begin{aligned}
T_{8,nf,x}^{(1)}(\Psi) = & T_{8,nf,x}^{(1)}(\eta_c) + \phi_\pi(x) \left\{ -\frac{2}{3}((C_A - 3)\log(1-x) - (C_A - 3)\log(x) + 8)\log\left(\frac{m_b^2}{\mu^2}\right) \right. \\
& + \log(z) \left(-\frac{2(2x-1)\log(2)C_A}{3(x-1)x} + \frac{16(x-1)x\log(1-x) - 16(x-1)x\log(x) + 36x\log(2) - 18\log(2)}{9(x-1)x} \right) \\
& \left. + \frac{C_A}{18(x-1)x} f_{17} + \frac{1}{18(x-1)x} f_{18} \right\}, \tag{121}
\end{aligned}$$

with

$$\begin{aligned}
f_7 = & \log(x)(4(2x^2-3x+1)^2\log(x+1) + (x+3)(2x-1)^3 + 8x(x-1)^3\log(2-x) \\
& - 2(4x(x(5x-9)+5) - 3)(x-1)\log(2)),
\end{aligned}$$

$$\begin{aligned}
f_8 = & \log(1-x)(x(x(-4x(x+5) + 8x(5x-9)\log(2) + 37+38\log(2)) - 19-4\log(2)) \\
& + 2(x-1)x(-\log(x+1) - 4(x-1)x(2\log(2-x) + \log(x+1))) + 3),
\end{aligned}$$

$$\begin{aligned}
f_9 = & 24x^3\log(2)\log(4-2x) - 8x(x^3+3x-1)\log(2)\log(2-x) + x(4x^3(13\log(2)-28) - 8x^2(-29+3\log^2(2)+8\log(2)) \\
& + 15x(\log(2)-12) + 62+8\log(2)) - \pi^2(x-1)^2 + 8x(x-1)^3\log^2(1-x) + 2x(x(-4(x-3)x-13) + 6)\log^2(x) \\
& - 2\log^2(x) + 4i\pi(x-1)^2\log(2) + (2x(x(x(\log(16)-16) + 8-12\log(2)) + 12+13\log(2)) \\
& - 2(5+3\log(2))) + 2\log(2))\log(x+1) + 4\log(x+1) - 8-3\log(2),
\end{aligned}$$

$$\begin{aligned}
f_{10} = & (16x(x-1)^4\log(2-x) + 4(2x-1)^3(x-1)^2\log(x+1) - 2x(x-1)(2x(2x(4x-8-7\log(2)) + 10+17\log(2)) \\
& - 3(2+5\log(2))) + 2(1-2x)^2(x(4x-1)+1)(x-1)\log(2x+1) + 1+2\log(2)),
\end{aligned}$$

$$\begin{aligned}
f_{11} = & (-32x^2(x-1)^3\log(2-x) - 2x(2x-1)^3(x-1)\log(x+1) + x(x(4x(x(20x-37-20\log(2)) \\
& + 29+30\log(2)) - 51-52\log(2)) + 12+\log(16)) - 1),
\end{aligned}$$

$$\begin{aligned}
f_{12} = & (-(x-2)x(2x-1)(3x-2)(8x^2-6x+3)\log(1-\frac{x}{2}) + \log(1-x)(-32x^6\log(4-2x) \\
& + 32(2x(x(2x-3)+2) - 1)x^2\log(2-x) + x(x(4x(x(4x(5+2\log(2)) - 57 \\
& - 20\log(2)) + 66+50\log(2)) - 167-172\log(2)) + 7(9+8\log(2))) - 13-4\log(2)) \\
& - 2(x-1)^2(2x-1)^3x\log(x+1) + 1) - 2(x-1)x(x(4x-1)+1)(1-2x)^2\log(x)\log(2x+1)),
\end{aligned}$$

$$\begin{aligned}
f_{13} = & (x(6(x(72x^2 - 62x - 23) + 41) - 13)(2x - 1)\log(2) + 8(47x - 20)(2x - 1)^3 - 3\pi^2(x(8x(x(20x - 47) + 39) \\
& - 101) + 8) + 36(x(2x(2x(2x(x + 3) - 17) + 29) - 23) + 4)\log^2(2)) + 18(16x^2(x - 1)^4\log^2(1 - x) \\
& + x((1 - 2x)^2((2x - 1)(-6(x^2 - 1)\log^2(\frac{x+1}{2}) + (-2(x - 2)x - 3)\log^2(x) + 2(x - 1)^2\log(2)\log(x + 1)) \\
& + 2x((5 - 4x)x - 2) + 1)\log(x)\log(2x + 1)) - (x - 2)(3x - 2)(8x^2 - 6x + 3)(2x - 1)\log(1 - \frac{x}{2}) \\
& + 6(x - 2)x(2x - 1)^3\log^2(1 - \frac{x}{2})) + (x - 1)\log(1 - x)(-32x^2(x - 1)^3\log(2 - x) \\
& - 2x(2x - 1)^3(x - 1)\log(x + 1) + x(x(4x(x(20x - 37 - 20\log(2)) + 29 + 30\log(2)) - 51 \\
& - 52\log(2)) + 12 + \log(16)) - 1)) - 288x^2(x - 1)^4\log(2)\log(4 - 2x)),
\end{aligned}$$

$$\begin{aligned}
f_{14} = & (x(180x - 58x\log(2) - 139 + 40\log(2)) - 2((x - 1)x + 2)\log(1 - x) + 2((x - 1)x + 2)\log(2 - x) \\
& + 64(x - 1)x\log(2x) - 2 - 4\log(2)),
\end{aligned}$$

$$\begin{aligned}
f_{15} = & (x(x^2\log(128x) - 32(x - 1)x\log(2 - 2x) + (3 - 4x)\log(2x) - (x - 3)(x - 1)\log(x + 1)) \\
& + x(x(15 + 22\log(2)) - 9 - 28\log(2)) - 9 + 3),
\end{aligned}$$

$$\begin{aligned}
f_{16} = & (13\log(2)(\log(32) - 6x^2) + x(384x - 380 + (19 - 117\log(2))\log(2)) + 20 - 30\log(2)) + 5\pi^2(12x - 7) \\
& + 6\log^2(x) - 324\log^2(\frac{x+1}{2}) + 6(64(x - 1)x\log^2(1 - x) + 2x(-27(x - 2)\log^2(1 - \frac{x}{2}) + 4(9 - 8x)\log^2(x) \\
& + 27x\log^2(\frac{x+1}{2})) - 2((x - 1)x + 2)\log(2)\log(2 - x) + (2x((x - 4)\log(2) + 16) \\
& + 6\log(2))\log(x + 1)) + 192\log(x + 1),
\end{aligned}$$

$$\begin{aligned}
f_{17} = & (-6(x - 1)x\log^2(1 - x) + 6(x - 1)x\log^2(x) + 2(2x - 1)(\pi^2 - 3\log^2(2)) \\
& + 24(x - 1)x\log(2)\log(1 - x) - 24(x - 1)x\log(2)\log(x)),
\end{aligned}$$

$$\begin{aligned}
f_{18} = & 32(x - 1)x\text{Li}_2(\frac{x-1}{x}) - 32(x - 1)x\text{Li}_2(\frac{x}{x-1}) - 192x^2 - 46x^2\log^2(1 - x) + 46x^2\log^2(x) \\
& + 64x^2\log(2 - 2x)\log(1 - x) - 72x^2\log(2)\log(1 - x) - 48x^2\log(1 - x) + 72x^2\log(2)\log(x) - 48x^2\log(x) \\
& - 64x^2\log(x)\log(2x) - 10\pi^2x + 160x + 46x\log^2(1 - x) - 46x\log^2(x) + 28x\log^2(2) - 64x\log(2 - 2x)\log(1 - x) \\
& + 72x\log(2)\log(1 - x) + 64x\log(1 - x) - 72x\log(2)\log(x) + 16x\log(x) + 64x\log(x)\log(2x) \\
& + 8x\log(2)\log(2) - 44x\log(2) - 16\log(1 - x) + 4\pi^2 - 18\log^2(2) + 12\log(2) + 32\log(2).
\end{aligned}$$

And the integrated results

$$\begin{aligned}
T_{\text{nf},0}^{(1)}(\eta_c) = & \{6\log(\frac{m_b^2}{\mu^2}) + \frac{1}{24}(144\log(2) + 83\pi^2\log(2) - 162\log^2(2) - 48\log^3(2) - 29\pi^2\log(3) - 48\log(2)\log(3) \\
& - 60\log^2(2)\log(3) - 24\log(2)\log^2(3) + 34\log^3(3)) + \frac{1}{144}(-72 - 567\pi^2 - 144\pi^2\log(2) + 288\log^3(2) \\
& + 18\pi^2\log(3) + 1152\log(2)\log(3) + 288\log^2(2)\log(3) - 108\log^3(3) - 432\text{Li}_2(-2) - 72\log(2)\text{Li}_2(-2) \\
& - 792\text{Li}_2(-\frac{1}{2}) - 36\log(3)\text{Li}_2(\frac{1}{9}) + 360\log(3)\text{Li}_2(\frac{1}{3}) - 288\log(2)\text{Li}_2(\frac{2}{3}) + 288\log(3)\text{Li}_2(\frac{2}{3}) \\
& - 144i\pi\text{Li}_2(\frac{4}{3}) + 72\log(\frac{4}{3})\text{Li}_2(\frac{4}{3}) + 1076\text{Li}_2(2) + 792\log(2)\text{Li}_2(2) + 864\text{Li}_2(3) \\
& - 72\log(2)\text{Li}_2(3) + 252\text{Li}_2(4) + 72\text{Li}_3(-3) - 144\text{Li}_3(-\frac{1}{3}) + 72\text{Li}_3(\frac{1}{9}) + 72\text{Li}_3(\frac{1}{3}) \\
& + 288\text{Li}_3(\frac{2}{3}) - 72\text{Li}_3(\frac{4}{3}) - 432\text{Li}_3(2) + 216\text{Li}_3(3) - 72\text{Li}_3(9) + 36\zeta(3))\},
\end{aligned} \tag{122}$$

$$T_{\text{nf},0}^{(1)}(\Psi) = T_{\text{nf},0}^{(1)}(\eta_c), \tag{123}$$

$$\begin{aligned}
T_{\text{nf},8}^{(1)}(\eta_c) = & \{\frac{1}{3}(-11C_A + 16N_c + 2n_f - 6)\log(\frac{m_b^2}{\mu^2}) + (9\log z + 1)C_F + \frac{1}{72C_A}f_{19} + \frac{C_A}{72}f_{20} \\
& - \frac{2}{9}n_f(-3\log z - 4 + 3\log 2) - \frac{8(3 + \log(2))}{3}\log z + \frac{1}{108}f_{21}\},
\end{aligned} \tag{124}$$

$$T_{\text{nf},8}^{(1)}(\Psi) = T_{\text{nf},8}^{(1)}(\eta_c) - \frac{16}{3}\log(\frac{m_b^2}{\mu^2}) + \frac{1}{9}(3\pi^2 - 22(2 + 3\log(2))), \tag{125}$$

with

$$\begin{aligned}
f_{19} = & -292 - 252 \log^3(2) - 756 \log^3(3) + 36 \log^2(2)(20 + 7 \log(3)) + \pi^2(48 - 1071 \log(2) + 966 \log(3)) \\
& + 8 \log(2)(68 + 27 \log(3)(-2 + 7 \log(3))) - 126 \log(3) \text{Li}_2\left(\frac{1}{9}\right) - 18(-12 + 7 \log(2)) \text{Li}_2\left(\frac{1}{4}\right) \\
& - 1008 \log\left(\frac{3}{2}\right) \text{Li}_2\left(\frac{2}{3}\right) - 252(2 \log(2) + \log(3)) \text{Li}_2\left(\frac{4}{3}\right) + 36(-12 + 7 \log(2) + 21 \log(3)) \text{Li}_2(3) \\
& - 6i\pi(21 \text{Li}_2\left(\frac{1}{9}\right) + 42 \text{Li}_2\left(\frac{1}{4}\right) - 84 \text{Li}_2\left(\frac{4}{3}\right) + 42 \text{Li}_2(3)) - 1008 \text{Li}_3\left(\frac{2}{3}\right) + 252 \text{Li}_3\left(\frac{4}{3}\right) \\
& - 1260 \text{Li}_3(3) + 63 \text{Li}_3(9) + 1197 \zeta(3), \tag{126}
\end{aligned}$$

$$\begin{aligned}
f_{20} = & (250 + 64 \log(2) + 60 \log^3(2) + 18 \log(2) \log^2(3) + 6(36 - 17 \log(3)) \log^2(3) + 72 \log^2(2)(-5 + 2 \log(3)) \\
& + 3\pi^2(83 \log(2) - 22(29 + 5 \log(3))) + 36i(\pi + i \log(3)) \text{Li}_2\left(\frac{1}{9}\right) + 54(-4 + 2i\pi + \log(2)) \text{Li}_2\left(\frac{1}{4}\right) \\
& + 36(12 + 6i\pi - \log(18432)) \text{Li}_2\left(\frac{2}{3}\right) + 72(-3i\pi + \log\left(\frac{4}{3}\right)) \text{Li}_2\left(\frac{4}{3}\right) - 180 \text{Li}_3\left(-\frac{1}{3}\right) - 72 \text{Li}_3\left(\frac{4}{3}\right) \\
& + 288 \text{Li}_3\left(\frac{3}{2}\right) + 180 \text{Li}_3(3) + 27 \text{Li}_3(9) - 342 \zeta(3)), \tag{127}
\end{aligned}$$

$$\begin{aligned}
f_{21} = & (486 + 9\pi^2(731 - 80 \log(2)) + 216 \log(2) - 144(2 \log^2(2) + \log\left(\frac{4}{3}\right) \log(3)) + 288 \text{Li}_2\left(\frac{1}{3}\right) \\
& - 144 \text{Li}_2(4) - 12i\pi(24 \text{Li}_2\left(\frac{1}{9}\right) - 132 \text{Li}_2\left(\frac{1}{3}\right) + 6 \text{Li}_2(4))), \tag{128}
\end{aligned}$$

E The NLO B_c to charmonia transition form factors

Following, the QCD NLO B_c to charmonium transition form factors are given under leading power of m_c/m_b . We define $z = m_c/m_b$, $s = \frac{m_b^2}{m_b^2 - q^2}$ and $\gamma = \frac{m_b^2 - q^2}{4m_b m_c}$.

$$\begin{aligned}
\frac{f_+^{NLO}(q^2)}{f_+^{LO}(q^2)} = & 1 + \frac{\alpha_s}{4\pi} \left\{ \frac{1}{3} (11C_A - 2n_f) \log\left(\frac{\mu^2}{2\gamma m_c^2}\right) - \frac{10n_f}{9} + \frac{(\pi^2 - 6 \log(2))(s-1) + 3s \log(\gamma)}{6s+3} \right. \\
& + \frac{C_A}{72s^2 - 18} \left(18s^2(2s-1) \log^2(s) + 18(8 \log(2)s^3 - 2 \log(2)s^2 - 5 \log(2)s + s \right. \\
& + 2 \log(2)) \log(s) + (2s-1)(268s + \pi^2(6s^2 - 3s - 6) + 170) - 9(2s \\
& - 1) \log(\gamma)(\log(\gamma)s - (2 + 2 \log(2))s + 4 \log(2)) + 18(2s-1)(4s^2 + s \\
& - 2) \text{Li}_2(1-2s) - 18(4s^3 - 5s + 2) \text{Li}_2(1-s) + 18(s(4s(s+1) - 11) \\
& \left. + 4) \log^2(2) - 36(5(s-1)s + 1) \log(2) \right) \\
& + \frac{C_F}{6(1-2s)^2(2s+1)} \left(-6(2(s-1)s-1) \log^2(s)(1-2s)^2 + 3 \log(\gamma)(23s \right. \\
& + (5s-2) \log(\gamma) - 4(s+1) \log(2) + 12)(1-2s)^2 - 12(4s^2 + s \\
& - 2) \text{Li}_2(1-2s)(1-2s)^2 + 12(s(2s+3) - 1) \text{Li}_2(1-s)(1-2s)^2 \\
& - (\pi - 2\pi s)^2(s(4s-19) + 4) + 3(-32 \log^2(2)s^4 - 4(69 + 2 \log(2)(-37 \\
& + 5 \log(2)))s^3 + 8(18 + \log(2)(-31 + 9 \log(2)))s^2 + (61 + 28 \log(2) \\
& - 26 \log^2(2))s + 12 \log(2) + 2 \log^2(2) - 32) + (6s(8s(s(-4 \log(2)s \\
& + 3 \log(2) + 3) + 2 \log(2) - 3) - 18 \log(2) + 7) + 24 \log(2)) \log(s) \left. \right\}, \tag{129}
\end{aligned}$$

$$\begin{aligned}
\frac{f_+^{NLO}(0)}{f_+^{LO}(0)} = & 1 + \frac{\alpha_s}{4\pi} \left\{ \frac{1}{3} (11C_A - 2n_f) \log\left(\frac{2\mu^2}{m_b m_c}\right) - \frac{10n_f}{9} - \frac{1}{3} \log(z) - \frac{2 \log(2)}{3} \right. \\
& + C_F \left(\frac{1}{2} \log^2(z) + \frac{10}{3} \log(2) \log(z) - \frac{35}{6} \log(z) + \frac{2 \log^2(2)}{3} \right. \\
& + 3 \log(2) + \frac{7\pi^2}{9} - \frac{103}{6} \left. \right) \\
& + C_A \left(-\frac{1}{6} \log^2(z) - \frac{1}{3} \log(2) \log(z) - \frac{1}{3} \log(z) + \frac{\log^2(2)}{3} \right. \\
& \left. \left. - \frac{4 \log(2)}{3} - \frac{5\pi^2}{36} + \frac{73}{9} \right) \right\}, \tag{130}
\end{aligned}$$

$$\begin{aligned}
\frac{f_0^{NLO}(q^2)}{f_0^{LO}(q^2)} = & 1 + \frac{\alpha_s}{4\pi} \left\{ \frac{1}{3} (11C_A - 2n_f) \log\left(\frac{\mu^2}{2\gamma m_c^2}\right) - \frac{10n_f}{9} + \frac{\log(\gamma)}{3} \right. \\
& + \frac{C_A}{36s-18} \left(-6\text{Li}_2(1-s)(1-2s)^2 + 6\log^2(2)(1-2s)^2 + 6s(2s-1)\log^2(s) \right. \\
& + (2s-1)(\pi^2(2s-3) + 146) + (12s\log(2)(4s-3) + 6\log(2) - 6)\log(s) \\
& \left. - 3(2s-1)\log(\gamma)(\log(4\gamma) - 2) + 6(8s^2 - 6s + 1)\text{Li}_2(1-2s) - 12s\log(2) \right) \\
& + \frac{C_F}{18(1-2s)^2(s-1)} \left(-6(s-1)(2s-3)\log^2(s)(1-2s)^2 \right. \\
& - 12(s-1)(4s-1)\text{Li}_2(1-2s)(1-2s)^2 + 24(s^2-1)\text{Li}_2(1-s)(1-2s)^2 \\
& - 6(-6s(2s(3s-8) + 11) + 2s(4s(s(4s-9) + 7) - 9)\log(2) + 2\log(2) + 13)\log(s) \\
& + (s-1)(3\log(\gamma)(3\log(\gamma) - 8\log(2) + 35)(1-2s)^2 - 24(s+2)\log^2(2)(1-2s)^2 \\
& \left. \left. - (2s-1)(546s + \pi^2(8s^2 - 34s + 15) - 279) + 24(s(43s-42) + 10)\log(2) \right) \right) \Big\}, \tag{131}
\end{aligned}$$

$$\frac{f_0^{NLO}(0)}{f_0^{LO}(0)} = \frac{f_+^{NLO}(0)}{f_+^{LO}(0)}, \tag{132}$$

$$\begin{aligned}
\frac{V^{NLO}(q^2)}{V^{LO}(q^2)} = & 1 + \frac{\alpha_s}{4\pi} \left\{ \frac{1}{3} (11C_A - 2n_f) \log\left(\frac{\mu^2}{2\gamma m_c^2}\right) - \frac{10n_f}{9} \right. \\
& - \frac{C_A}{36s-18} \left(9s(2s-1)\log^2(s) + 18(2s\log(2)(2s-1) + 1)\log(s) \right. \\
& + 3\pi^2(s+2)(2s-1) - 2s(-18\log^2(2)s + 9\log^2(2) + 45\log(2) + 134) \\
& + 9(2s-1)(\log(\gamma) - 3)\log(\gamma) + 18s(2s-1)(2\text{Li}_2(1-2s) - \text{Li}_2(1-s)) \\
& \left. + 63\log(2) + 134 \right) \\
& + \frac{C_F}{6(1-2s)^2(s-1)} \left(6(s^2-1)\log^2(s)(1-2s)^2 + 24(s-1)s\text{Li}_2(1-2s)(1-2s)^2 \right. \\
& + 3(2s(s(4s(4\log(2)s - 8\log(2) + 3) + 20\log(2) - 17) - 4\log(2) + 7) - 1)\log(s) \\
& + (s-1)(6\log(\gamma)(\log(\gamma) - 6\log(2) + 5)(1-2s)^2 + 6(2s-9)\log^2(2)(1-2s)^2 \\
& + (2s-1)(-204s + 2\pi^2(2s^2 + s - 1) + 105) + 6(s(68s-67) + 16)\log(2)) \\
& \left. \left. - 12(2s^2 - 3s + 1)^2\text{Li}_2(1-s) \right) \right\}, \tag{133}
\end{aligned}$$

$$\begin{aligned}
\frac{V^{NLO}(0)}{V^{LO}(0)} = & 1 + \frac{\alpha_s}{4\pi} \left\{ \frac{1}{3} (11C_A - 2n_f) \log\left(\frac{2\mu^2}{m_b m_c}\right) - \frac{10n_f}{9} \right. \\
& + C_F \left(\log^2(z) + 10\log(2)\log(z) - 5\log(z) + 9\log^2(2) \right. \\
& \left. + 7\log(2) + \frac{\pi^2}{3} - 15 \right) \\
& + C_A \left(-\frac{1}{2}\log^2(z) - 2\log(2)\log(z) - \frac{3}{2}\log(z) - 3\log^2(2) \right. \\
& \left. \left. - \frac{3\log(2)}{2} - \frac{\pi^2}{3} + \frac{67}{9} \right) \right\}, \tag{134}
\end{aligned}$$

$$\frac{A_1^{NLO}(q^2)}{A_1^{LO}(q^2)} = \frac{A_2^{NLO}(q^2)}{A_2^{LO}(q^2)} = \frac{V^{NLO}(q^2)}{V^{LO}(q^2)}, \tag{135}$$

$$\begin{aligned}
\frac{A_0^{NLO}(q^2)}{A_0^{LO}(q^2)} = & 1 + \frac{\alpha_s}{4\pi} \left\{ \frac{1}{3} (11C_A - 2n_f) \log\left(\frac{\mu^2}{2\gamma m_c^2}\right) - \frac{10n_f}{9} \right. \\
& + \frac{C_A}{72(s-1)s(2s-1)} \left(-9(s-1)s(2s-1)(2s+1) \log^2(s) - 9(2s(2s \log(2)(4s^2-9) \right. \\
& + 3) + 12 \log(2) - 3) - 4 \log(2) - 2) \log(s) + (s-1)(-18(2s-1) \log^2(2)(s(2s+9) - 4) \\
& - (2s-1)(s(3\pi^2(2s+9) - 608) + 36) - 9(2s-1) \log(\gamma)(2 \log(\gamma)s + 8 \log(2)s - 6s \\
& + \log(\gamma) - 4 \log(2) - 3) + 9(4s(13s-7) - 3) \log(2)) - 36(s(4s^3 - 9s + 6) - 1) \text{Li}_2(1-2s) \\
& \left. + 18(s-1)(2s-1)(s(2s+5) - 2) \text{Li}_2(1-s) \right) \\
& + \frac{C_F}{24s(2s^2-3s+1)^2} \left(2\pi^2(1-2s)^2(s(2s-1) + 3)(s-1)^2 \right. \\
& + 24(1-2s)^2(s(2s+3) - 1) \text{Li}_2(1-2s)(s-1)^2 + 6s(2s+5)(2s^2-3s+1)^2 \log^2(s) \\
& + 3(s(s(2s \log(2)(2s(76s-193) + 289) + 4s(-120s^2 + 369s + (8s^3 - 52s^2 + 90s - 43) \log^2(2) \\
& - 406) - 84 \log^2(2) - 28 \log(2) + 747) + 92 \log^2(2) - 110 \log(2) - 116) + 16 \log^2(2) \\
& + 4(7 - 9 \log(2)) \log(2) - 3) + 3(s(2s(s(2s(4s(4 \log(2)s - 6 \log(2) + 6) - 28 \log(2) - 69) \\
& + 156 \log(2) + 113) - 2(13 + 58 \log(2))) + 72 \log(2) - 5) - 8 \log(2) + 1) \log(s) \\
& - 6(2s^2 - 3s + 1)^2(16 \log(2)s - 22s - 2 \log(\gamma) + 4 \log(2) + 1) \log(\gamma) \\
& \left. - 12(2s^2 - 3s + 1)^2(2s^2 + s - 2) \text{Li}_2(1-s) \right) \}, \tag{136}
\end{aligned}$$

$$\begin{aligned}
\frac{A_0^{NLO}(0)}{A_0^{LO}(0)} = & 1 + \frac{\alpha_s}{4\pi} \left\{ \frac{1}{3} (11C_A - 2n_f) \log\left(\frac{2\mu^2}{m_b m_c}\right) - \frac{10n_f}{9} + C_F \left(\frac{1}{2} \log^2(z) - \frac{119}{8} \right. \right. \\
& + 7 \log(2) \log(z) - \frac{21}{4} \log(z) + 7 \log^2(2) + \frac{15 \log(2)}{4} \Big) \\
& + C_A \left(-\frac{3}{8} \log^2(z) - \log(2) \log(z) - \frac{9}{8} \log(z) - \frac{7\pi^2}{24} + \frac{67}{9} \right. \\
& \left. \left. - \frac{9 \log^2(2)}{4} + \frac{3 \log(2)}{8} \right) \right\}. \tag{137}
\end{aligned}$$

References

- [1] N. Brambilla, et al. (Quarkonium Working Group), CERN-2005-005, [arXiv:hep-ph/0412158].
- [2] F. Abe, et al. (CDF Collaboration), Phys. Rev. Lett. **81**, 2432 (1998).
- [3] V. M. Abazov et al. (D0 Collaboration), Phys. Rev. Lett. **101**, 012001(2008).
- [4] T. Aaltonen et al. (CDF Collaboration), Phys. Rev. Lett. **100**, 182002(2008).
- [5] A. Abulencia et al. (CDF Collaboration), Phys. Rev. Lett. **97**, 012002(2006).
- [6] V. M. Abazov et al. (D0 Collaboration), Phys. Rev. Lett. **102**, 092001(2009).
- [7] Y.-N. Gao, J.-B. He, P. Robbe, M.-H. Schune, Z.-W. Yang, Chin. Phys. Lett. **27**, 061302(2010).
- [8] R. Aaij et al. (LHCb Collaboration), Phys. Rev. Lett. **108**, 251802(2012), [arXiv:1204.0079].
- [9] C.-H. Chang, C. Driouichi, P. Eerola and X.-G. Wu, Comput. Phys. Commun. **159**, 192 (2004).
- [10] C.-H. Chang, and X.-G. Wu, Eur. Phys. J. C **38**, 267-276 (2004).
- [11] G. T. Bodwin, E. Braaten and G. P. Lepage, Phys. Rev. D **51**, 1125 (1995), [Erratum-ibid.D55:5853,1997].
- [12] G. Buchalla, A. J. Buras and M. E. Lautenbacher, Rev. Mod. Phys. **68**, 1125 (1996).

- [13] M. Beneke, G. Buchalla, M. Neubert and C. T. Sachrajda, Nucl. Phys. B **591**, 313 (2000).
- [14] T. Hahn, Comput. Phys. Commun, **140**, 418 (2001).
- [15] R. Mertig, M. Böhm, and A. Denner, Comput. Phys. Commun, **4**, 345 (1991).
- [16] T. Hahn and M. Perez-Victoria, Comput. Phys. Commun, **118**, 153 (1999).
- [17] J.G. Körner, D. Kreimer and K. Schilcher, Z. Phys. C **54**, 503 (1992)
- [18] C.-F. Qiao, L.-P. Sun and R.-L. Zhu, JHEP **1108**, 131 (2011).
- [19] M. Beneke, Th. Feldmann, Nucl. Phys. B **592**, 3-34 (2001).
- [20] V.M. Braun and I.E. Filyanov, Z Phys. C **48**, 239 (1990).
- [21] Guido Bell, Ph.D. Thesis, arXiv:0705.3133[hep-ph].
- [22] G. Bell and T. Feldmann, JHEP **0804**, 061 (2008).
- [23] C.-F. Qiao, P. Sun and F. Yuan, JHEP **1208**, 087 (2012), arXiv:1103.2025[hep-ph].
- [24] C.-F. Qiao and R.-L. Zhu, arXiv:1208.5916[hep-ph].
- [25] R. Keith Ellis and Giulia Zanderighi, JHEP **0802**, 002 (2008).
- [26] Stefan Dittmaier, Nucl. Phys. B **675**, 447 (2003).
- [27] M. Beneke and S. Jager, Nucl. Phys. B **751** (2006) 160 [arXiv:hep-ph/0512351].
- [28] M. Beneke, G. Buchalla, M. Neubert and C. T. Sachrajda, Phys. Rev. Lett. **83** (1999) 1914 [hep-ph/9905312].
- [29] M. Beneke, G. Buchalla, M. Neubert and C. T. Sachrajda, Nucl. Phys. B **591** (2000) 313 [hep-ph/0006124].
- [30] J.P. Ma and Z.G. Si, Phys. Lett. B **647**, 419(2007).
- [31] Y. Jia and D. Yang, Nucl. Phys. B **814**, 217(2009).
- [32] M. Beneke and D. Yang, Nucl. Phys. B **736**, 34-81 (2006).
- [33] Nikolai Kivel, JHEP **0705**, 019(2007).
- [34] Volker Pilipp, arXiv:0709.0497 [hep-ph].
- [35] K. Nakamura, et al, Particle Data Group, J. Phys. G **37**, 075021(2010).
- [36] E. J. Eichten and C. Quigg, Phys. Rev. D **49**, 5845-5856(1994).
- [37] V. V. Kiselev, A. E. Kovalsky and A. K. Likhoded, Nucl. Phys. B **585**, 353 (2000) [arXiv:hep-ph/0002127];
- [38] V. V. Kiselev, arXiv:hep-ph/0211021.
- [39] C. H. Chang and Y. Q. Chen, Phys. Rev. D **49**, 3399 (1994).
- [40] A. Y. Anisimov, P. Y. Kulikov, I. M. Narodetsky and K. A. Ter-Martirosian, Phys. Atom. Nucl. **62**, 1739 (1999) [Yad. Fiz. **62**, 1868 (1999)] [arXiv:hep-ph/9809249].

- [41] P. Colangelo and F. De Fazio, Phys. Rev. D **61**, 034012 (2000) [arXiv:hep-ph/9909423].
- [42] D. Ebert, R. N. Faustov and V. O. Galkin, Phys. Rev. D **68**, 094020 (2003) [arXiv:hep-ph/0306306].
- [43] A. Abd El-Hady, J. H. Munoz and J. P. Vary, Phys. Rev. D **62**, 014019 (2000) [arXiv:hep-ph/9909406].
- [44] M. A. Ivanov, J. G. Körner, P. Santorelli, Phys. Rev. D **73**, 054024 (2006).
- [45] Junfeng Sun, Dongsheng Du and Yueling Yang, Eur. Phys. J. C **60**, 107-117 (2009).
- [46] B. Aubert, et al. (BABAR Collaboration) Phys. Rev. Lett. **99**, 261801(2007).
- [47] K. C. Yang, Nucl. Phys. **B776**, 187(2007).
- [48] Hai-Yang Cheng and Sechul Oh, JHEP **1109**, 024 (2011); Guohuai Zhu, JHEP **1005**, 063 (2010).
- [49] Patricia Ball, V.M. Braun, Y. Koike and K. Tanaka, Nucl. Phys. B **529**, 323-382 (1998); C.-D. Lü, M.-Z. Yang, Eur.Phys.J. C **28**, 515-523 (2003).
- [50] E. Braaten, Phys. ReV. D **28**, 524 (1983).